Downloaded from rspb.royalsocietypublishing.org on May 13, 2014

PROCEEDINGS OF THE ROYAL SOCIETY B

rspb.royalsocietypublishing.org

Research

Cite this article: Kremer N, Schwartzman J, Augustin R, Zhou L, Ruby EG, Hourdez S, McFall-Ngai MJ. 2014 The dual nature of haemocyanin in the establishment and persistence of the squid–vibrio symbiosis. *Proc. R. Soc. B* **281**: 20140504.
http://dx.doi.org/10.1098/rspb.2014.0504

Received: 2 March 2014
Accepted: 2 April 2014

Subject Areas:
physiology, biochemistry, microbiology

Keywords:
haemocyanin, host–symbiont interaction, oxygen provision, specificity

Authors for correspondence:
Natacha Kremer
e-mail: natacha.kremer@normalesup.org
Margaret J. McFall-Ngai
e-mail: mjmcfallngai@wisc.edu

†Present address: Laboratoire de Biométrie et Biologie Evolutive, UMR CNRS 5558, Université Lyon 1, Villeurbanne, France.

Electronic supplementary material is available at http://dx.doi.org/10.1098/rspb.2014.0504 or via http://rspb.royalsocietypublishing.org.

Royal Society Publishing

The dual nature of haemocyanin in the establishment and persistence of the squid–vibrio symbiosis

Natacha Kremer[1,†], Julia Schwartzman[1], René Augustin[1], Lawrence Zhou[1], Edward G. Ruby[1], Stéphane Hourdez[2,3] and Margaret J. McFall-Ngai[1]

[1]Department of Medical Microbiology and Immunology, University of Wisconsin–Madison, Madison, WI, USA
[2]CNRS UMR 7144, Station Biologique de Roscoff, Roscoff, France
[3]UPMC Université Paris 06, Laboratoire Adaptation et Diversité en Milieu Marin, Roscoff, France

We identified and sequenced from the squid *Euprymna scolopes* two isoforms of haemocyanin that share the common structural/physiological characteristics of haemocyanin from a closely related cephalopod, *Sepia officinalis*, including a pronounced Bohr effect. We examined the potential roles for haemocyanin in the animal's symbiosis with the luminous bacterium *Vibrio fischeri*. Our data demonstrate that, as in other cephalopods, the haemocyanin is primarily synthesized in the gills. It transits through the general circulation into other tissues and is exported into crypt spaces that support the bacterial partner, which requires oxygen for its bioluminescence. We showed that the gradient of pH between the circulating haemolymph and the matrix of the crypt spaces in adult squid favours offloading of oxygen from the haemocyanin to the symbionts. Haemocyanin is also localized to the apical surfaces and associated mucus of a juvenile-specific epithelium on which the symbionts gather, and where their specificity is determined during the recruitment into the association. The haemocyanin has an antimicrobial activity, which may be involved in this enrichment of *V. fischeri* during symbiont initiation. Taken together, these data provide evidence that the haemocyanin plays a role in shaping two stages of the squid–vibrio partnership.

1. Introduction

The bobtail squid *Euprymna scolopes* establishes a light organ symbiosis with the luminous bacterium *Vibrio fischeri*. During embryogenesis, the host develops ciliated epithelial tissues on the surface of the nascent organ that, after the host hatches, promote both the harvesting of the symbiont cells from the seawater and their eventual colonization of the organ's deep tissues. After hatching, these superficial epithelia shed mucus, and ciliary-mucus currents entrain the bacterioplankton into regions above pores, through which the symbionts will enter the organ. *Vibrio fischeri* and other Gram-negative bacteria adhere to the cilia and aggregate in mucus near the pores; however, by approximately 3 h, *V. fischeri* has become the only resident of these aggregates, i.e. specificity of the symbiosis is determined on the surface, even before the symbiont enters the host [1].

The mechanisms underlying this specificity have not been well defined. However, several lines of data suggest that the biochemistry of the microenvironment plays a critical role. For example, antimicrobials such as nitric oxide (NO) [2] and a peptidoglycan-recognition protein (*Es*PGRP2), which breaks down bacterial cell walls, are present in the mucus [3]. Resistance to NO is critical for the ability of *V. fischeri* to colonize normally [4]. Further, recent analyses have shown that interaction with as few as three to five *V. fischeri* cells, which are bound to the cilia on the light organ surface during initiation of the association, induce changes in host gene expression [5], including the upregulation of those predicted to encode antimicrobial proteins that may be critical for determining specificity [5].

Vibrio fischeri cells that reach the crypts grow and, after attaining a critical density, begin to luminesce using host-derived nutrients and oxygen [6,7].

© 2014 The Author(s) Published by the Royal Society. All rights reserved.

Downloaded from rspb.royalsocietypublishing.org on May 13, 2014

Key features of the symbiosis express profound diel rhythms; first, the symbiont population density dramatically varies over the day, i.e. approximately 95% of the bacteria are expelled from the light organ at dawn and the remaining bacteria subsequently repopulate the crypts. Second, symbiont light production also fluctuates during the day, increasing during the evening and peaking early at night [8]. Experiments manipulating the rhythm suggest that, even though the symbionts reach their maximum density during the day, the production of bioluminescence is limited by oxygen availability in the crypts until later during the night [8].

The relationships of the adult light organ tissues [9] suggest that the diffusion of oxygen from the surrounding seawater is unlikely to match the symbionts' needs. Further, the light organ is one of the most highly vascularized regions of the host's body, suggesting that oxygen is delivered to the symbionts through the circulatory system [10]. In the squid, and certain other invertebrates, the metalloprotein haemocyanin, which is dissolved in the haemolymph, transports oxygen throughout the body; oxygen binding in haemocyanins is cooperative, and its affinity can be affected by pH, temperature and various solutes [11]. A recent study of the squid–vibrio system demonstrated that the genes encoding the host's haemocyanin are regulated over the day–night cycle in the adult tissues that support the symbiont [12]. These data suggested a role for haemocyanin in the dynamics of the mature symbiosis.

Haemocyanins arose from ancestral copper-coordinating proteins, which had diverged into two protein families, the tyrosinases and the pro-phenol oxidases; the former gave rise to the haemocyanin of molluscs, and the latter to the haemocyanin of arthropods [13,14]. Thus, despite their common mechanism of oxygen binding, their separate origins resulted in structural and functional distinctions. Specifically, arthropod haemocyanin isoforms have one functional unit (FU), while the molluscan haemocyanin isoforms comprise seven to eight FUs, whose three-dimensional conformation slightly differs from that of the arthropods [15].

Apart from oxygen binding, the protein domains of the mollusc haemocyanins also have two distinct phenol oxidase (PO) activities: a cresolase, which hydrolyses monophenol into *o*-diphenols and is specific to tyrosinases, and a catechol oxidase, which oxidizes *o*-diphenols [15]. These enzymatic activities can be enhanced *in vitro* by proteolytic treatment or the use of detergents [15]. This proteolytic enhancement also occurs *in vivo* in crustaceans, with the activation of immune defence pathways in response to the recognition of bacterial products [15,16]. As such, the PO activity plays a role in controlling microbial pathogenesis through the production of highly reactive quinones.

In this study, we characterize biochemical features of the host haemocyanin and provide evidence for a role for this protein in the regulation of the mature light organ, as well as in the initial establishment of the symbiosis. We first describe the primary structure of haemocyanin. We next show that, in addition to being the major respiratory protein in the blood, haemocyanin co-occurs with the symbiont cells within the crypts and delivers oxygen to these regions of the organ. Finally, our *in vitro* data suggest that, through its PO activity, haemocyanin participates in the creation of an antimicrobial cocktail that selects for *V. fischeri* during initiation of the symbiosis.

2. Material and methods

(a) General procedures

Adult Hawaiian bobtail squid (*E. scolopes*) were caught in Oahu, Hawaii and transported to UW-Madison, where they were maintained and bred in a recirculating seawater system. Juvenile squid were incubated overnight either in the absence of *V. fischeri* (aposymbiotic) or in the presence of approximately 10^5 CFU ml^{-1} of either the wild-type *V. fischeri* strain ES114 (WT) or a deletion mutant derivative defective in light production, Δ*luxCDABEG* (Δ*lux*) [17]. All animal protocols followed regulatory standards established by UW-Madison.

Microscope observations were either performed on a Zeiss 510 laser-scanning confocal or a Zeiss Axio Imager M2 epifluorescence microscope. Unless otherwise noted, all chemicals were purchased from Sigma-Aldrich (USA) and all molecular reagents and fluorochromes from Life Technologies (USA). Primers (electronic supplementary material, table T1), which were synthesized by Integrated DNA Technologies (USA), and buffer formulae are defined in the electronic supplementary material.

(b) Analysis of the cDNA

Full-length cDNA sequences of HCY isoforms (GenBank accession numbers KF647897 and KF647898) were obtained by rapid-amplification of cDNA ends (RACE), using the GeneRacer kit, following the manufacturer's instructions (for details, see the electronic supplementary material, Material and methods).

We aligned full-length haemocyanin cDNA from a variety of mollusc species (electronic supplementary material, Material and methods) using MUSCLE v. 3.7 [18], and conserved sites were selected using GBLOCKS v. 0.91b [19]. Maximum-likelihood reconstruction was performed using PHYML v. 3.0 [20] with the WAG + Γ model, and 100 bootstrap replicates were conducted for support estimation (Dryad doi:10.5061/dryad.cq032). We used the interface from phylogeny.fr as a platform for the reconstruction [21].

Haemocyanin transcripts from both isoforms were quantified by quantitative reverse-transcription PCR (qRT-PCR) using specific transcripts for each isoform. The qRT-PCR protocol, previously described in [5], followed the MIQE guideline [22] ($n = 4$ replicates of one adult or 20 juveniles). For specifics, see the electronic supplementary material, Material and methods. *In situ* hybridization against *haemocyanin2* transcripts was performed as described in [5].

(c) Protein localization

An affinity-purified polyclonal antibody (α-HCY2) was produced in chicken against the synthetic peptide CISFDNSETDRDPQP (GenScript, USA). Soluble proteins from juvenile light organs, extracted in phosphate-buffered saline (PBS) containing a protease inhibitor cocktail, were separated on a 7% SDS-polyacrylamide gel for western blot analysis as described in [5] (see the electronic supplementary material, Material and methods for details).

Immunocytochemistry (ICC) experiments on whole light organs were performed as previously described [3], with either the primary α-HCY2 antibody or α-IgY as a negative control, at a dilution of 1 : 1000 for 7 days (see the electronic supplementary material, Material and methods for details). ICC experiments in mucus were performed as before [3], except that squid were fixed for 3 h in Bouin's solution, permeabilized for 2 h in a marine PBS (mPBS) containing Triton X100 (mPBST), and the mucus was counterstained with Alexa633-wheatgerm agglutinin (WGA).

ICC experiments on paraffin sections were performed as follows: squid were fixed in 4% paraformaldehyde in mPBS overnight at 4°C and embedded in paraffin. Five-micrometre sections were deparaffinized in histoclear solution (National Diagnostics) and rehydrated in an ethanol series. Slides were brought to

Downloaded from rspb.royalsocietypublishing.org on May 13, 2014

boiling in the antigen retrieval solution (RD Systems), then cooled to 65°C and incubated for 10 min. Slides were then rinsed in deionized water followed by mPBS and blocked in mPBS containing 0.5% BSA and 1% goat serum for 30 min at room temperature (RT). Slides were incubated in α-HCY2 or α-IgY antibodies 1 : 500 in the blocking solution overnight at 4°C and rinsed 3 × 5 min in mPBS. Slides were then incubated in blocking solution for 1 min, then for 1 h at RT in a goat-anti-chicken, FITC-conjugated secondary antibody diluted in blocking solution. Slides were rinsed 3 × 15 min in mPBS and counterstained for actin with 1 : 40 rhodamine phalloidin in mPBS overnight at 4°C, and for nuclei with a 1 : 1000 dilution of TOTO-3 for 10 min at RT. Slides were then mounted in Vectashield (Vector Laboratories), and samples were viewed by confocal microscopy.

(d) Determination of oxygen affinity

For oxygen affinity measurements, collected haemolymph samples were either: (i) used directly in a diffusion chamber apparatus, or (ii) the haemocyanin was separated from the small metabolites and smaller proteins present in the haemolymph by two passages through an Amicon Ultra-4 with Ultracel-100 membrane (Millipore) in 2 × 3.5 ml of stabilization buffer III and concentrated to the same volume as that of the initial haemolymph sample. The functional measurements were made in a diffusion chamber, using a step-by-step procedure, as previously described [23]. Five microlitres of the native sample, or of the 'purified' samples adjusted at different pH values (pH approx. 6.5, 7.0, 7.5, 7.8 and 8.0), were equilibrated in the chamber with pure N_2, pure O_2 and mixtures of the two gases to determine the oxygen equilibrium curves. The Bohr effect Φ, which characterizes the relationship between oxygen binding affinity and pH, was determined by the equation $\Phi = \Delta\log P_{50}/\Delta pH$. For details about the determination of oxygen affinity, see the electronic supplementary material, Material and methods.

(e) Protein purification, and the determination of phenol oxidase and antimicrobial activities

Haemolymph samples were centrifuged at 2000 × *g* for 10 min at 4°C to pellet haemocytes. Next, to remove small molecules, haemolymph was filtered three times through an Amicon Ultra-4 with Ultracel-100 membrane (Millipore) in 3.5 ml of stabilization buffer I. The remaining haemocyanin protein was pelleted by centrifugation overnight at 25 000 × *g* at 4°C. The pellet was resuspended in stabilization buffer II and passed through an anion-exchange chromatography column (MonoQ 4.6/100 PE, GE Healthcare) for high-performance liquid chromatography (HPLC). Buffer A and buffer B were run as a linear gradient from 0 to 100% B in A using over 80 column volumes at a flow rate of 1 ml min^{-1}. Fractions absorbing at 560 nm were collected and exchanged two times with stabilization buffer I using the Amicon column as described above. Before storage at −80°C, these purified (more than 95%) haemocyanin extracts were pooled and concentrated to 66 mg protein ml^{-1}, as calculated spectrophotometrically as: $C = (A_{235} - A_{280})/2.51 \times$ dilution factor [24].

PO activity of haemocyanin was determined based on the method described in [16] with some modifications. Briefly, 66 µg of purified haemocyanin was diluted in a PIPES-based buffer (pH 6.3) to obtain a final volume of 123 µl. Also, depending on the combination tested (figure 4*a*), 40 µg of protease (subtilisin Karlsberg, type XIV protease or cathepsin L) and/or 1 mM phenylthiourea (PTU) was added. Reactions were then incubated in microplate wells for 10 min at RT, and 2 µl of dopamine, catechol or tyramine was added to final concentrations of 6, 6 and 3.4 mM, respectively. In triplicate experiments, quinone production was recorded at 420 nm (Tecan spectrophotometer, GENios) after a 1-h (or 3.5-h, for tyramine) incubation at RT.

To determine the lowest concentration of haemocyanin that inhibits the growth of different marine bacterial strains, a modified minimal inhibitory concentration (MIC) test was performed as described in [25]. Briefly, a dilution series of purified haemocyanin in PIPES buffer [16] containing 625 µM dopamine as substrate was placed into wells containing 100 bacterial colony-forming units (CFU). For each series, the presence or absence of bacterial growth (i.e. a circular pellet appearing at the bottom of the well) was recorded after 24 h of incubation at 28°C (see the electronic supplementary material, Material and methods, for details). No bactericidal activity was observed in the presence of dopamine alone.

(f) Characterization of flow between the haemolymph and the light organ crypts, and measurement of pH

After anaesthesia, adult squid were injected in the cephalic vessel with 50 µl of a 1 : 100 dilution of the fluorescent pH indicator carboxy-SNARF-4F [5] in seawater, or a seawater-only control. Following injection, the squid were revived and maintained for at least 12 h prior to assay. To monitor SNARF accumulation in the light organ crypts, the crypt contents (vented material) were collected as described previously [10]. A fluorescent SNARF signal was detected in the expelled contents of SNARF-injected, but not carrier-injected, animals using epifluorescence microscopy. The pH of haemolymph and expelled crypt contents was measured as described previously [5], except by epifluorescence. Briefly, the probe was excited at 488 nm and emission was measured at two different wavelengths (580 and 650 nm); the emission ratio depends on the pH of the solution. A pH calibration curve was obtained with 20 independently measured ratios from a series of 5 pH standards made with SNARF in mPBS.

3. Results and discussion

(a) *Euprymna scolopes* synthesizes two isoforms of haemocyanin

(i) Haemocyanin structure

The derived amino acid sequence of RACE products revealed two distinct isoforms of haemocyanin (*Es*HCY), consisting of 3342 and 3346 amino acids that share 80% identity. Each isoform comprised eight FUs, originating from ancestral duplication events, and sharing the ABCDD'EFG subunit organization first described in *Sepia officinalis* [26,27] (figure 1; electronic supplementary material, figure S1).

The two isoforms diverged before the split between the cephalopod orders Sepiida and Sepiolida. An analogous duplication event occurred independently in the gastropods, before the divergence of keyhole limpets and abalones. Each FU of both isoforms has retained its oxygen-binding residues, i.e. the essential histidine that coordinates copper in type-3 centres A and B [13]. The comparison of *Es*FU-G with the crystal structure of FU-G in *Octopus dofleini* [28–30] supports the structural conservation of this domain, particularly in the inner α-helixes, where the functional residues are located. Because the haemocyanin FU organization of *E. scolopes* is very similar to that of *S. officinalis*, we can predict its three-dimensional structure, based on crystallographic analyses of the cuttlefish's [27,31]: specifically, the subunits of the *S. officinalis* haemocyanin form a large cylindrical decamer that resembles a wall and collar, and that has a more compact appearance than that of other cephalopod haemocyanins.

Downloaded from rspb.royalsocietypublishing.org on May 13, 2014

(*a*)

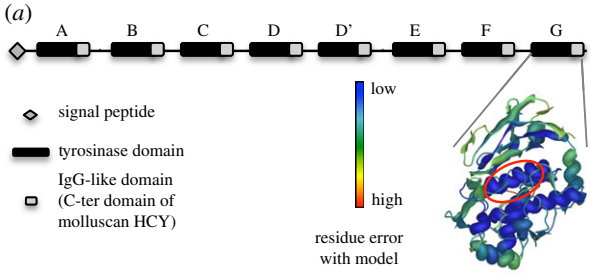

(*b*)

molluscan class	subtaxon	genus	no. isoforms	no. subunits	subunit organization
Gastropoda	Vetigastropoda	*Megathura*	2	8	ABCDEFGH
Gastropoda	Vetigastropoda	*Haliotis*	2	8	ABCDEFGH
Gastropoda	Euopisthobranchia	*Aplysia*	1	8	ABCDEFGH
Bivalvia	Protobranchia	*Nucula*	2	8	ABCDEFGH
Cephalopoda	Nautiloidea	*Nautilus*	1	7	ABCDEFG
Cephalopoda	Octopodiformes	*Octopus*	2	7	ABCDEFG
Cephalopoda	Decapodiformes	*Sepia*	2	8	ABCDD'EFG
Cephalopoda	Decapodiformes	*Euprymna*	2	8	ABCDD'EFG

(*c*)

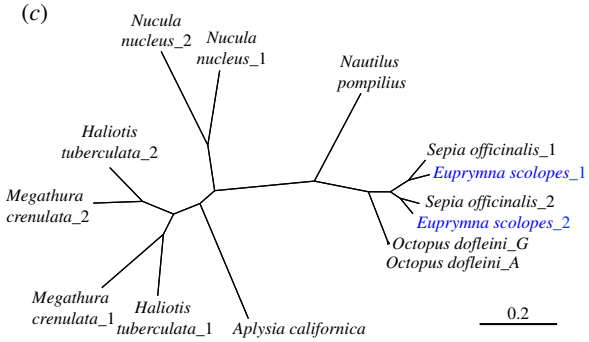

Figure 1. Characterization of haemocyanin from *E. scolopes*. (*a*) Schematic of *Es*HCY. Right: illustration of the predicted three-dimensional structure of FU-G of HCY2 against crystal structures from *O. dofleini* (Od-G; Swiss-Prot model (FU-G): 1js8B [28]); catalytic centre circled in red; colour scale indicates error level. *Z*-scores values, representing the deviation of the *Es*HCY's FU-G structures from that of the authentic crystal structure, are −1.4 and −0.64 for HCY1 and HCY2, respectively, with a percentage of BLAST sequence identity of 72.5 and 74.6%. $Z = 0$ for the crystal; valid models vary from −4 to +4 [29]. (*b*) Characteristics of haemocyanin proteins from different mollusc species. (*c*) Maximum-likelihood inference phylogeny based on haemocyanin sequences from different mollusc species. All nodes had a bootstrap value more than 99 (100 replicates).

(ii) Haemocyanin synthesis and expression

We quantified the expression of mRNA encoding each haemocyanin isoform by quantitative RT-PCR and localized the transcripts by *in situ* hybridization in both juvenile and adult squid tissues (figure 2*b*,*c*). These mRNAs were mainly synthesized in the gills, with particularly strong labelling in the branchial gland, as previously described in other cephalopods [32]. Secondary sites of synthesis were detected in the mantle and gut of juvenile squid, as well as in the eyes and symbiont-containing central core of the light organ of adult squid. Both isoforms were expressed at similar levels in all tissues. However, these data did not eliminate the possibility that fine-scale differences in localization of the two isoforms could occur.

We used an antibody to *Es*HCY (α-HCY2) to define the fine-scale distribution of the protein in host tissues (figure 2*e*–*k*). Because haemocyanin is secreted and transported, protein localization is likely to differ from sites of gene transcription. The antibody reacted against a protein at the predicted size of *Es*HCY (expected monomeric molecular weight: 382 kDa) both in the haemolymph (data not shown) and in the light organ (figure 2*d*). Confocal analyses of the ICC with α-HCY2 revealed cross-reactivity in the gills and epithelia of the juvenile light organ (figure 2*e*–*g*). In addition, cross-reactive sites localized to the mucus adjacent to the ciliated epithelium (figure 2*h*). Thus, although gene expression was low in the ciliated epithelia, the protein was abundant, suggesting either (i) *Es*HCY is highly stable and, despite its low synthesis rate, can accumulate in the tissues; or (ii) the protein is transported from the blood sinus into the epithelial cells by transcytosis. Precedence for the latter hypothesis is supported by studies in *S. officinalis*, in which haemocyanin occurs in the intercellular space, and in vesicles and vacuoles of the renal and branchial epithelia, a phenomenon initially attributed to a possible role for haemocyanin in copper homoeostasis [33]. *Es*HCY was also detectable in the adult central core, mainly in the crypt epithelium but also in the crypt spaces, where symbionts are located (figure 2*j*,*k*). These results are consistent with the proteomic detection of haemocyanin in crypt contents [34]. By ICC, we could not detect an influence of symbiosis (WT versus aposymbiotic) or symbiont bioluminescence (WT versus Δ*lux*) on the pattern of haemocyanin production in the light organ (electronic supplementary material, figure S3). However, these methods are insufficiently sensitive to discount the possibility that small differences occur between these conditions.

(b) Vascular haemocyanin provides oxygen to symbionts in the crypt space

The oxygen-binding properties of squid haemocyanin were determined using whole-blood samples collected from adult animals at different times during the day (figure 3) and were in the range reported for other cephalopod haemocyanins [35]. Specifically, blood samples collected during the night had a pH of 7.16 ± 0.08, and a P_{50} for oxygen, i.e. pressure at which haemocyanin is half-saturated with oxygen, of 1.62 ± 0.25 kPa, with a cooperativity coefficient of 2.43 ± 0.10 at 26°C. By contrast, samples collected during the day had a pH of 6.94 ± 0.04, a significantly decreased affinity (P_{50} of 5.40 ± 1.58 kPa), but an essentially unchanged cooperativity coefficient (2.67 ± 0.14). These values are equivalent to a half-saturation of 18 µM during the night and 61 µM during the day and indicate that at both times *Es*HCY has an oxygen affinity two to three orders of magnitude lower than the nanomolar values reported for *V. fischeri* luciferase and cytochromes [36]. These results indicate that haemocyanin helps deliver oxygen from the haemolymph to the symbionts to support the elevated oxygen demand of luminescence.

The squid's alternating behaviours of hiding in the sand (day) and hunting in the water column (night) may differentially influence blood pH [37] and, thus, *Es*HCY's oxygen affinity through a Bohr effect. To determine the extent of this effect, we separated *Es*HCY from other blood components by repeated exchange with a Tris-based buffer adjusted to pH values between 6.0 and 8.2. Subsequent measurements indicated the protein's oxygen affinity (figure 3*b*), but not cooperativity (electronic supplementary material, figure S4*a*), was strongly reduced by a lower pH, with an observed Bohr effect of −0.76, typical of cephalopods [38] and other invertebrates [39]. Oxygen affinity decreased after the haemocyanin

Downloaded from rspb.royalsocietypublishing.org on May 13, 2014

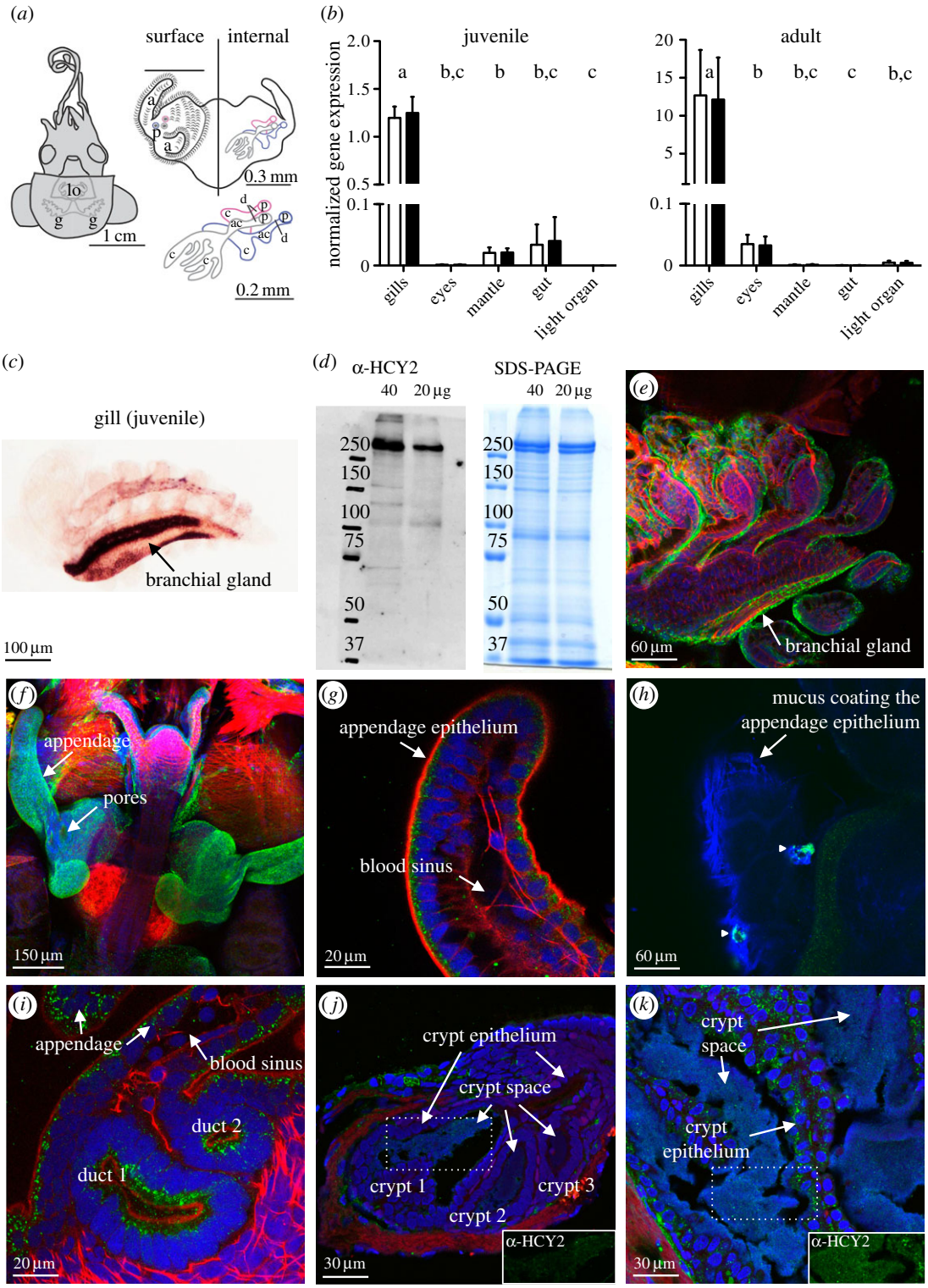

Figure 2. Localization of haemocyanin transcript and protein in squid tissues. (*a*) Left: ventral surface of the squid showing the gills (g) and the light organ (lo) deep in the mantle cavity. Right, top: enlargement of the light organ, showing the muco-ciliary epithelial surfaces (ce) in contact with seawater, as well as the internal features (enlarged below) through which *V. fischeri* cells pass during their migration to the crypts. a, appendage; ac, antechamber; c, crypt; d, duct; p, pore. (*b*) Normalized gene expression of *Eshcy1* (white bars) and *Eshcy2* (black bars) in different tissues from juvenile ($n = 4 \times 20$ animals) and adult ($n = 4$ animals) squid, as mean $\pm$ s.e. In this set of comparisons, those pairs of bars that share letters are not significantly different, statistically (ANOVA with Tukey honestly significant difference (HSD) adjustment for pairwise comparisons). (*c*) *In situ* hybridization showing the strong staining of the *Eshcy2* riboprobe in the gills, where cephalopods typically produce haemocyanin. (*d*) Coomassie staining of a 7% SDS-PAGE gel (right) of soluble protein (20 and 40 µg samples) extracted from juvenile light organs, and its associated western blot (left) against *Es*HCY antibody (α-HCY2); expected size of the monomer: 383 kDa. (*e–i*) ICC of *Es*HCY2 in juvenile tissues. The antigen labelling is particularly bright in the gills (*e*), and in the ciliated field (*f*), the cytosol of the appendage epithelium (*g*) and the pore/duct regions (*i*) of the light organ. Green, α-HCY2 (antibody); red, rhodamine phalloidin (f-actin); blue, TOTO-3 (nuclei). (*h*) ICC of *Es*HCY2 in the mucus coating the appendage epithelium. Triangles indicate foci of α-HCY2 cross-reactivity in the mucus. Green, α- HCY2; blue, Alexa633-WGA (mucus-binding lectin, WGA). (*j–k*) ICC of *Es*HCY2 in 5-µm sections of symbiotic juvenile (*j*) and adult (*k*) light organs. In both samples, antigen labelling is present in the lumen of the crypt space, in direct contact with bacteria. Green, α-HCY2; red, rhodamine phalloidin (f-actin); blue, TOTO-3 (nuclei). The inset shows α-HCY2 staining (green channel only) corresponding to the dotted area. Negative controls for the ISH (sense probe), western blot and ICC, are presented in the electronic supplementary material, figure S2. In all cases, these control tissues/extracts showed no detectable labelling.

Downloaded from rspb.royalsocietypublishing.org on May 13, 2014

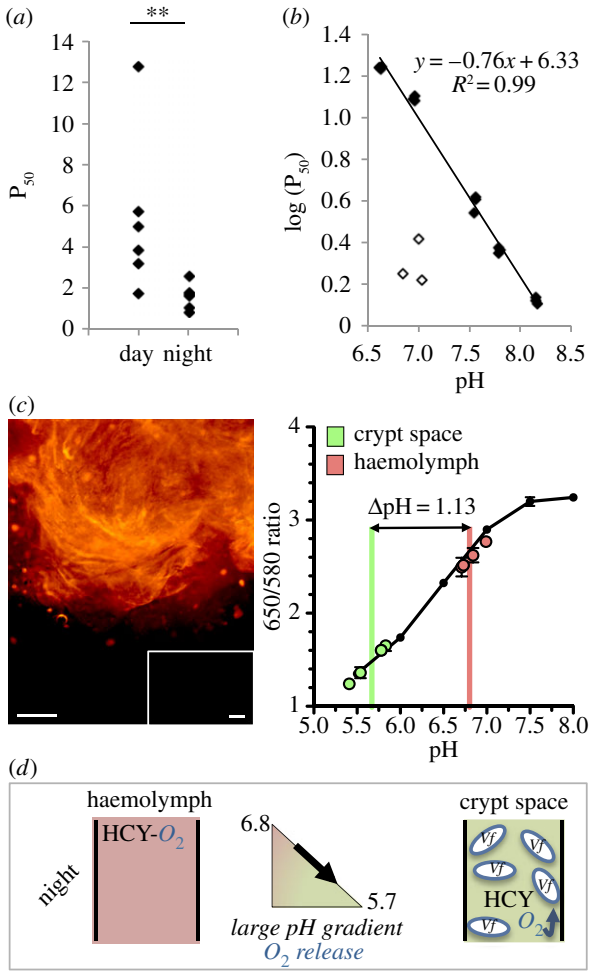

Figure 3. Characteristics of the haemocyanin protein and its putative role in the delivery of oxygen to the symbionts. (*a*) The affinity for oxygen in native haemolymph samples is lower during the day (14.00–16.00; $n = 6$) than during the night (2.00–4.00; $n = 6$). P_{50} in kPa. $^{**}p < 0.01$ based on a Wilcoxon's test. (*b*) Determination of the Bohr effect of *Es*HCY using the regression between log(P_{50}) and pH. Oxygen affinity of the *Es*HCY samples was measured after exchanging it in five stabilization buffers at pHs of approximately 6.5, 7.0, 7.5, 7.8 or 8.0 (closed diamonds). Affinity was also measured in native (unprocessed) haemolymph samples (open diamonds). (*c*) Circulation between the haemolymph and the crypt space, and the associated pH values. The pH-sensitive dye SNARF was injected into the cephalic artery and transported through the body. SNARF is excited at 488 nm, and selectively emits at two different wavelengths (580 and 650 nm). The 650/580 ratio is characteristic of a particular pH, which is estimated by a calibration curve, generated in pH-adjusted mPBS. SNARF was detected in the central core of the light organ (image, left). Injection with sterile seawater revealed no autofluorescence (inset). The pH was determined both in the circulating haemolymph and in the crypt space, i.e. expelled material, in adult squid during the night (figure, right; mean ± s.e., $n = 5$). Scale bars, 100 µm. (*d*) A model for the directional transport of oxygen into the crypt space during the night. During the night, circulating haemocyanin (left), which has a relatively high oxygen affinity, circulates to and enters the crypt spaces that have become acidic as a result of bacterial metabolism. The reduced pH in the crypts favours the offloading of oxygen from the haemocyanin (right) to the symbionts, where it is used by their high-affinity luciferase.

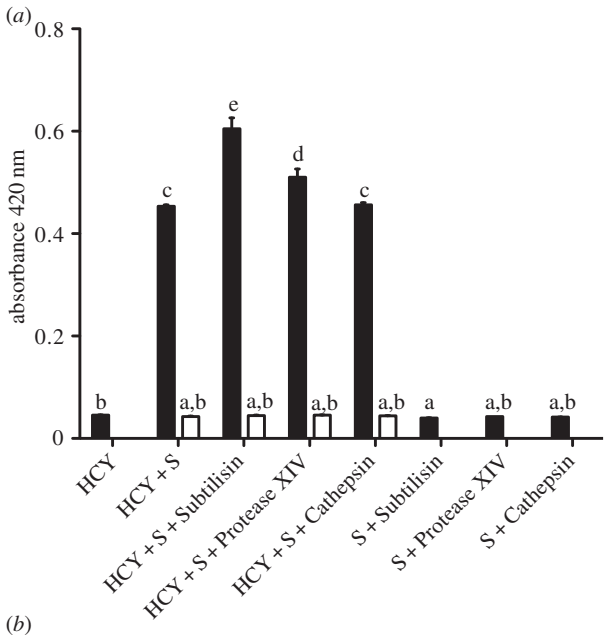

(*b*)

bacterial species	name	Gram	MIC (µM)
Vibrio azureus-like	NK_St13	–	0.02
Photobacterium leognathi	Lna	–	0.3
Bacillus algicola-like	CNJ 803	+	0.6
Vibrio fischeri	ES114	–	1.2
Bacillus megaterium-like	CNJ 778	+	4.8
Exiguobacterium aestuarii-like	CNJ 771	+	9.6
Vibrio parahaemolyticus	KNH1	–	>9.6

Figure 4. Antimicrobial properties of haemocyanin. (*a*) Determination of the PO activity of *Es*HCY (HCY). The reaction's absorbance was measured spectrophotometrically after a 1-h incubation in the presence of 6 mM dopamine substrate (S) and/or different proteases. White bars correspond to the PO-activity in the presence of the inhibitor (1 mM PTU). Mean ± s.e. ($n = 3$). Different letters indicate a statistical difference between samples (ANOVA with Tukey HSD adjustment for pairwise comparisons). (*b*) Minimal inhibitory concentration (MIC) of haemocyanin against various Gram-negative and Gram-positive bacterial strains in the presence of 625 µM dopamine in a PIPES-based buffer at pH 6.35.

was separated from the other blood components (electronic supplementary material, figure S4*b*); however, addition of candidate blood components produced by the squid (taurine) or the symbionts (acetate and lactate) had no detectable effect on *Es*HCY oxygen affinity (electronic supplementary material, figure S4*c*).

These results led to an investigation of whether a pH gradient between the blood and the crypt spaces might affect oxygen delivery by haemocyanin to the symbionts. Haemocyanin is present in the crypt space of symbiotic light organs (figure 2; electronic supplementary material, figure S3); however, whether this haemocyanin comes from the circulating blood is unclear. Therefore, we tested whether haemocyanin travels from the general circulation to the crypt space and measured the associated pH values at those two sites. We injected into the cephalic artery a pH-sensitive fluorescent probe (SNARF), which does not permeate membranes by diffusion. We showed that (i) the light organ is highly vascularized, (ii) haemolymph passes from the vascular system into the crypt space and (iii) the pH is significantly lower in the crypt than the haemolymph (5.67 ± 0.18 versus 6.80 ± 0.12) (figure 3*c*). These data suggest that haemocyanin-bound oxygen taken up in the gills and transported in the haemolymph may be effectively offloaded into the acidic crypt spaces (figure 3*d*). The consumption of oxygen by *V. fischeri* (including that driving more than 10% of the cell's energy commitment going to bioluminescence [40]) will thus presumably

Downloaded from rspb.royalsocietypublishing.org on May 13, 2014

lead to a gradient that requires a constant flow of oxygen into the crypts.

Bacterial transcriptomic profiles and metabolic modelling [12,36] collectively support the prediction that changes in symbiont, rather than host [37], metabolism over the day–night cycle may influence the pH of the crypt spaces and, thereby, the delivery of oxygen. Thus, we hypothesize that oxygen-saturated vascular haemocyanin migrates to the crypt spaces where a 1-unit pH differential (figure 3*c*) lowers its affinity for oxygen, driving the oxygen towards the high-affinity, high-demand activity of the symbiont's luciferase (figure 3*d*). Hence, a combination of *Es*HCY biochemistry and symbiont metabolism may work together to promote bioluminescence in the squid crypts.

The squid–vibrio system is not unique in recruiting an oxygen-carrier metalloprotein for the control of symbiont activities. In the nodules of legumes, oxygen is provided to symbionts *via* leghaemoglobin. This carrier poises the levels of oxygen in symbiotic tissues, providing optimal conditions for the activity of symbiont nitrogenase [41]; however, it can also sanction rhizobium cells whose nitrogen-fixation efficiency is low, by limiting their growth [42]. In hydrothermal vent and cold seep tubeworms [43], haemoglobins play a role in delivery of both oxygen and hydrogen sulfide to the symbiotic tissue [44]. In the squid–vibrio association, the haemocyanin provides both respiratory oxygen to host tissues and oxygen for bacterial light production, which is the basis of the symbiosis; in contrast, in tubeworms, it is the sulfide that allows its symbionts to fix carbon, which is 'the currency' of that symbiosis.

(c) Haemocyanin antimicrobial activity is linked to phenol oxidase activity

Haemocyanin is part of the tyrosinase family of enzymes [14] and exhibits a PO including tyrosinase activity in certain taxa [45]. The production of quinones by the PO activity is antimicrobial [16,46]. Thus, because haemocyanin is present in mucus coating the ciliated epithelium of the light organ, where symbionts are recruited and selected from the bacterioplankton (figure 2), we hypothesized that haemocyanin also has an antimicrobial function during these initial events. Therefore, we purified haemocyanin from squid haemolymph using size-exclusion and anion-exchange HPLC separation (see the electronic supplementary material, figure S5*a*). The PO activity of this purified protein was determined using dopamine, an *o*-diphenol common in cephalopods, especially in the adjacent ink sac. We characterized the PO activity in an acidic buffer mimicking the mucus pH, and in the presence/absence of several proteases that could enhance the PO activity [15,16]. Haemocyanin exhibited significant PO activity using dopamine as the substrate and, similar to arthropod and molluscan haemocyanins whose PO activity is enhanced by proteases [16,47], *Es*HCY exhibited a higher PO activity in the presence of certain proteases, particularly a subtilisin-type bacterial serine-protease with broad specificity towards proteins (figure 4*a*). This activation might be linked to the cleavage of either the N- or C-terminus of the protein or to a conformation change that opens a substrate-binding pocket [45]. Similar results were obtained using other substrates for PO, such as catechol, another *o*-diphenol and tyramine, a mono-phenol, for which slower kinetics were observed. These results showed that *Es*HCY has a catecholase activity and, to a lesser extent, a cresolase activity, typical of tyrosinases (see the electronic supplementary material, figure S5*b*). Contrary to the PO activity of crustacean haemocyanins [16], the PO activity of *Es*HCY was not affected by the presence of LPS (the ratio of dopamine-based activity with/without *Vf*-LPS was 1.07; *t*-test, $p = 0.08$).

To test whether the PO activity of *Es*HCY is antimicrobial, we determined the minimal concentration of haemocyanin required to inhibit growth of various strains of marine bacteria in the presence of dopamine. *Vibrio fischeri* exhibited an intermediate resistance compared with other marine Gram-negative and Gram-positive strains tested (figure 4*b*). In addition, when we assayed the antimicrobial activity of unpurified blood, which potentially contains proteases, but without the addition of dopamine, no antimicrobial activity was detected (data not shown). These results suggest that the main antimicrobial activity of haemocyanin is linked to its PO activity. Taken together, the data suggest that the *Es*HCY protein, which is secreted into the mucus, could play a role in the selection of the symbiont, perhaps in combination with other antimicrobial factors, e.g. NO, PGRP2, lysozymes [2,3,5], that occur in the mucus matrix.

4. Conclusion

The data presented here suggest a role for haemocyanin in the dynamics of the squid–vibrio symbiosis, both in its initiation and its maintenance. We showed that haemocyanin exhibits antimicrobial properties that, in combination with other antimicrobials present in the mucus, may be involved in selecting *V. fischeri* during harvesting. The synergistic mechanisms between these various antimicrobials remain to be determined, but promise to provide valuable insight into how specificity is achieved even before symbionts enter host tissues. This activity might also be critical for controlling symbionts throughout the life of the animal, e.g. by limiting growth of the symbionts, preventing colonization by non-specific bacteria or even sanctioning cheaters. Determining whether *Es*HCY has these functions will require further study.

We are beginning to develop a clearer concept of the elements of the squid–vibrio system that are controlled on a diel rhythm, and how they are regulated. Earlier studies showed a day–night cycle on features ranging from bacterial bioluminescence to gene expression [8,12], and recently this symbiosis was the first in which the bacteria were found to drive host circadian rhythms [48]. Our data reveal the possibility that haemocyanin is an important component of these rhythms, at least in the adult animal. Our current model for how the symbiosis modulates oxygen delivery for luminescence by the microbial partner relies in part on the pH gradient between haemolymph and the crypt environment. The capacity of the symbiont to lower the crypt pH favours the release of oxygen from haemocyanin, and host provision of nutrients is likely to have a profound influence on the symbiont's ability to modulate pH in these tissues. Not unlike the host–symbiont conversation that goes on during the establishment of the association [5], the permanent adjustment of the partners' biochemistry and physiology may play a critical role in the maintenance of the symbiosis as well.

Acknowledgement. N.K., M.J.M-N. and E.G.R. conceived and designed the study. N.K. performed all the experiments and data analyses, except the blood circulation experiment (J.S.) and a preliminary

Downloaded from rspb.royalsocietypublishing.org on May 13, 2014

experiment for dopamine sensitivity (L.Z.). R.A. helped with the experimental design of protein purification and antimicrobial activity. S.H. was involved in the design and supervision of the oxygen affinity experiments. N.K., M.J.M-N. and E.G.R. wrote the manuscript. All the authors have read and approved the final version of the manuscript.

Funding statement. This work was supported by the Marie Curie Actions FP7-PEOPLE-2010-IOF/272684/SymbiOx to N.K., NSF Graduate Research Fellowship and NIH NIGMS T32 GM008505 to J.S., NIH grant nos. AI 50661 to M.J.M-N. and OD 011024 to E.G.R. and M.J.M-N., and the Region Bretagne HYPOXEVO research programme to S.H.

References

1. Nyholm SV, McFall-Ngai MJ. 2004 The winnowing: establishing the squid–vibrio symbiosis. *Nat. Rev. Microbiol.* **2**, 632–642. (doi:10.1038/nrmicro957)
2. Davidson SK, Koropatnick TA, Kossmehl R, Sycuro L, McFall-Ngai MJ. 2004 NO means 'yes' in the squid–vibrio symbiosis: nitric oxide (NO) during the initial stages of a beneficial association. *Cell. Microbiol.* **6**, 1139–1151. (doi:10.1111/j.1462-5822.2004.00429.x)
3. Troll JV, Bent EH, Pacquette N, Wier AM, Goldman WE, Silverman N, McFall-Ngai MJ. 2010 Taming the symbiont for coexistence: a host PGRP neutralizes a bacterial symbiont toxin. *Environ. Microbiol.* **12**, 2190–2203. (doi:10.1111/j.1462-2920.2009.02121.x)
4. Wang Y, Dunn AK, Wilneff J, McFall-Ngai MJ, Spiro S, Ruby EG. 2010 *Vibrio fischeri* flavohaemoglobin protects against nitric oxide during initiation of the squid–vibrio symbiosis. *Mol. Microbiol.* **78**, 903–915. (doi:10.1111/j.1365-2958.2010.07376.x)
5. Kremer N *et al*. 2013 Initial symbiont contact orchestrates host-organ-wide transcriptional changes that prime tissue colonization. *Cell Host Microbe* **14**, 183–194. (doi:10.1016/j.chom.2013.07.006)
6. Ruby EG, McFall-Ngai MJ. 1999 Oxygen-utilizing reactions and symbiotic colonization of the squid light organ by *Vibrio fischeri*. *Trends Microbiol.* **7**, 414–420. (doi:10.1016/S0966-842X(99)01588-7)
7. Stabb EV. 2005 Shedding light on the bioluminescence 'paradox'. *ASM News* **71**, 223–229.
8. Boettcher KJ, Ruby EG, McFall-Ngai MJ. 1996 Bioluminescence in the symbiotic squid *Euprymna scolopes* is controlled by a daily biological rhythm. *J. Comp. Physiol. A* **179**, 65–73. (doi:10.1007/BF00193435)
9. McFall-Ngai MJ, Montgomery MK. 1990 The anatomy and morphology of the adult bacterial light organ of *Euprymna scolopes* Berry (Cephalopoda: Sepiolidae). *Biol. Bull.* **179**, 332–339. (doi:10.2307/1542325)
10. Nyholm SV, Stewart JJ, Ruby EG, McFall-Ngai MJ. 2009 Recognition between symbiotic *Vibrio fischeri* and the haemocytes of *Euprymna scolopes*. *Environ. Microbiol.* **11**, 483–493. (doi:10.1111/j.1462-2920.2008.01788.x)
11. Decker H, Hellmann N, Jaenicke E, Lieb B, Meissner U, Markl J. 2007 Minireview: recent progress in hemocyanin research. *Integr. Comp. Biol.* **47**, 631–644. (doi:10.1093/icb/icm063)
12. Wier AM *et al*. 2010 Transcriptional patterns in both host and bacterium underlie a daily rhythm of anatomical and metabolic change in a beneficial symbiosis. *Proc. Natl Acad. Sci. USA* **107**, 2259–2264. (doi:10.1073/pnas.0909712107)
13. Van Holde KE, Miller KI, Decker H. 2001 Hemocyanins and invertebrate evolution. *J. Biol. Chem.* **276**, 15 563–15 566. (doi:10.1074/jbc.R100010200)
14. Martín-Durán JM, de Mendoza A, Sebé-Pedrós A, Ruiz-Trillo I, Hejnol A. 2013 A broad genomic survey reveals multiple origins and frequent losses in the evolution of respiratory hemerythrins and hemocyanins. *Genome Biol. Evol.* **5**, 1435–1442. (doi:10.1093/gbe/evt102)
15. Decker H, Jaenicke E. 2004 Recent findings on phenoloxidase activity and antimicrobial activity of hemocyanins. *Dev. Comp. Immunol.* **28**, 673–687. (doi:10.1016/j.dci.2003.11.007)
16. Jiang N, Tan NS, Ho B, Ding JL. 2007 Respiratory protein-generated reactive oxygen species as an antimicrobial strategy. *Nat. Immunol.* **8**, 1114–1122. (doi:10.1038/ni1501)
17. Bose JL, Rosenberg CS, Stabb EV. 2008 Effects of *luxCDABEG* induction in *Vibrio fischeri*: enhancement of symbiotic colonization and conditional attenuation of growth in culture. *Arch. Microbiol.* **190**, 169–183. (doi:10.1007/s00203-008-0387-1)
18. Edgar RC, Drive RM, Valley M. 2004 MUSCLE: multiple sequence alignment with high accuracy and high throughput. *BMC Bioinform.* **32**, 1792–1797. (doi:10.1093/nar/gkh340)
19. Castresana J. 2000 Selection of conserved blocks from multiple alignments for their use in phylogenetic analysis. *Mol. Biol. Evol.* **17**, 540–552. (doi:10.1093/oxfordjournals.molbev.a026334)
20. Guindon S, Gascuel O. 2003 A simple, fast, and accurate algorithm to estimate large phylogenies by maximum likelihood. *Syst. Biol.* **52**, 696–704. (doi:10.1080/10635150390235520)
21. Dereeper A *et al*. 2008 Phylogeny.fr: robust phylogenetic analysis for the non-specialist. *Nucleic Acids Res.* **36**, W465–W469. (doi:10.1093/nar/gkn180)
22. Bustin S *et al*. 2009 The MIQE guidelines: minimum information for publication of quantitative real-time PCR experiments. *Clin. Chem.* **55**, 611–622. (doi:10.1373/clinchem.2008.112797)
23. Weber RE. 1981 Cationic control of O_2 affinity in lugworm erythrocruorin. *Nature* **292**, 386–387. (doi:10.1038/292386a0)
24. Whitaker JR, Granum PE. 1980 An absolute method for protein determination based on difference in absorbance at 235 and 280nm. *Anal. Biochem.* **109**, 156–159. (doi:10.1016/0003-2697(80)90024-X)
25. Fedders H, Leippe M. 2008 A reverse search for antimicrobial peptides in *Ciona intestinalis*: identification of a gene family expressed in hemocytes and evaluation of activity. *Dev. Comp. Immunol.* **32**, 286–298. (doi:10.1016/j.dci.2007.06.003)
26. Lamy J, You V, Taveau JC, Boisset N, Lamy JN. 1998 Intramolecular localization of the functional units of *Sepia officinalis* hemocyanin by immunoelectron microscopy. *J. Mol. Biol.* **284**, 1051–1074. (doi:10.1006/jmbi.1998.2235)
27. Markl J. 2013 Evolution of molluscan hemocyanin structures. *Biochim. Biophys. Acta* **1834**, 1840–1852. (doi:10.1016/j.bbapap.2013.02.020)
28. Cuff ME, Miller KI, van Holde KE, Hendrickson WA. 1998 Crystal structure of a functional unit from *Octopus* hemocyanin. *J. Mol. Biol.* **278**, 855–870. (doi:10.1006/jmbi.1998.1647)
29. Benkert P, Biasini M, Schwede T. 2011 Toward the estimation of the absolute quality of individual protein structure models. *Bioinformatics* **27**, 343–350. (doi:10.1093/bioinformatics/btq662)
30. Arnold K, Bordoli L, Kopp J, Schwede T. 2006 The SWISS-MODEL workspace: a web-based environment for protein structure homology modelling. *Bioinformatics* **22**, 195–201. (doi:10.1093/bioinformatics/bti770)
31. Boisset N, Mouche F. 2000 *Sepia officinalis* hemocyanin: a refined 3D structure from field emission gun cryoelectron microscopy. *J. Mol. Biol.* **296**, 459–472. (doi:10.1006/jmbi.1999.3460)
32. Schipp R, Höhn P, Ginkel G. 1973 Elektronenmikroskopische und histochemische Untersuchungen zur Funktion der Branchialdriise (Parabranchialdrtise) der Cephalopoda. *Z. Zellforsch.* **139**, 253–269. (doi:10.1007/BF00306525)
33. Beuerlein K, Westermann B, Ruth P, Schimmelpfennig R, Schipp R. 2000 Hemocyanin re-uptake in the renal and branchial heart appendages of the coleoid cephalopod *Sepia officinalis*. *Cell Tissue Res.* **301**, 413–421. (doi:10.1007/s004 410000254)
34. Schleicher TR, Nyholm SV. 2011 Characterizing the host and symbiont proteomes in the association between the bobtail squid, *Euprymna scolopes*, and the bacterium, *Vibrio fischeri*. *PLoS ONE* **6**, e25649. (doi:10.1371/journal.pone.0025649)
35. Melzner F, Mark FC, Pörtner H-O. 2007 Role of blood-oxygen transport in thermal tolerance of the cuttlefish, *Sepia officinalis*. *Integr. Comp. Biol.* **47**, 645–655. (doi:10.1093/icb/icm074)
36. Dunn AK. 2012 Vibrio fischeri *metabolism: symbiosis and beyond*, 1st edn. Elsevier, The Netherlands: Elsevier Ltd.
37. Pörtner H-O. 1994 Coordination of metabolism, acid–base regulation and haemocyanin function in

Downloaded from rspb.royalsocietypublishing.org on May 13, 2014

cephalopods. *Mar. Freshw. Behav. Physiol.* **25**, 131–148. (doi:10.1080/10236249409378913)

38. Pörtner H-O. 1990 An analysis of the effects of pH on oxygen binding by squid (*Illex illecebrosus, Loligo pealei*) hemocyanin. *J. Exp. Biol.* **424**, 407–424.
39. Van Holde KE, Miller KI. 1995 Hemocyanins. *Adv. Prot. Chem.* **47**, 1–81. (doi:10.1016/S0065-3233(08)60545-8)
40. Karl DM, Nealson KH. 1980 Regulation of cellular metabolism during synthesis and expression of the luminous system in *Beneckea* and *Photobacterium*. *J. Gen. Microbiol.* **117**, 357–368. (doi:10.1099/00221287-117-2-357)
41. Bergersen FJ. 1997 Regulation of nitrogen fixation in infected cells of leguminous root nodules in relation to O_2 supply. *Plant Soil* **191**, 189–203. (doi:10.1023/A:1004236922993)
42. Kiers ET, Rousseau RA, West SA, Denison RF. 2003 Host sanctions and the legume–rhizobium mutualism. *Nature* **425**, 78–81. (doi:10.1038/nature01931)
43. Childress JJ, Girguis PR. 2011 The metabolic demands of endosymbiotic chemoautotrophic metabolism on host physiological capacities. *J. Exp. Biol.* **214**, 312–325. (doi:10.1242/jeb.049023)
44. Flores JF, Hourdez SM. 2006 The zinc-mediated sulfide-binding mechanism of hydrothermal vent tubeworm 400-kDa hemoglobin. *Cah. Biol. Mar.* **47**, 371–377.
45. Decker H, Schweikardt T, Nillius D, Salzbrunn U, Jaenicke E, Tuczek F. 2007 Similar enzyme activation and catalysis in hemocyanins and tyrosinases. *Gene* **398**, 183–191. (doi:10.1016/j.gene.2007.02.051)
46. Cerenius L, Lee BL, Söderhäll K. 2008 The proPO-system: pros and cons for its role in invertebrate immunity. *Trends Immunol.* **29**, 263–271. (doi:10.1016/j.it.2008.02.009)
47. Decker H, Tuczek F. 2000 Tyrosinase/catecholoxidase activity of hemocyanins: structural basis and molecular mechanism. *Trends Biochem. Sci.* **25**, 392–397. (doi:10.1016/S0968-0004(00)01602-9)
48. Heath-Heckman EAC, Peyer SM, Whistler CA, Apicella MA, Goldman WE, McFall-Ngai MJ. 2013 Bacterial bioluminescence regulates expression of a host cryptochrome gene in the squid–vibrio symbiosis. *mBio* **4**, e00167–13. (doi:10.1128/mBio.00167-13)

Supplementary material

The dual nature of hemocyanin in the establishment and persistence of the squid-vibrio symbiosis

Natacha Kremer, Julia Schwartzman, René Augustin, Lawrence Zhou, Edward G. Ruby, Stéphane Hourdez, Margaret J. McFall-Ngai

Supplementary Material and Methods

(a) General methods

Squid were bred in a recirculating seawater system of filter-sterilized Instant Ocean (Aquarium Systems) (FSIO), and maintained at 24 °C on a 12 h/12 h light/dark cycle. Before sacrifice, squid were anesthetized in 2 % ethanol, and either frozen for protein work or placed in RNA later until use. Hemolymph was withdrawn from the adult squid cephalic artery, as described in [3].

Vibrio fischeri strains used in colonisations were the wild-type (WT) strain, ES114 [1], and a mutant derivative defective in light production, ES114 ΔluxCDABEG (*Δlux*) [2]. For inoculations, bacteria were grown in LBS medium (Luria Bertani with 2 % wt/vol NaCl) with shaking at 28 °C to an OD_{600nm} 0.2-0.4, and diluted in FSIO to a final concentration of ~10^5 CFU/mL. The presence or absence of colonisation was assessed by monitoring bioluminescence (Turner 20/20 luminometer) and/or plating homogenates of the squid light organ on LBS agar plates to enumerate bacterial colonies.

Unless otherwise noted, all chemicals were purchased from Sigma-Aldrich (USA) and all molecular reagents and fluorochromes from Life Technologies (USA).

(b) Buffer composition

- marine Phosphate Buffered Saline (mPBS): 50 mM sodium phosphate pH 7.4, 0.45 M NaCl.
- marine Phosphate Buffered Saline-Triton (mPBST): 50 mM sodium phosphate pH 7.4, 0.45 M NaCl containing 1% Triton-X100.
- Buffer A (for HPLC): 20 mM Tris, pH 8
- Buffer B (for HPLC): 20 mM Tris, 1 M NaCl, pH 8

- Stabilisation buffer I: 100 mM Tris, 375 mM NaCl, 10 mM $CaCl_2$, 45 mM $MgCl_2$, 10 mM KCl, pH 8.

- Stabilisation buffer II: 50 mM Tris, 150 mM NaCl, 5 mM $CaCl_2$, 5 mM $MgCl_2$, pH 7.4.

- Stabilisation buffer III: 25 mM Tris, 375 mM NaCl, 14.7 mM $CaCl_2$, 60 mM $MgCl_2$, 15 mM KCl, pH 7.

- Tris Buffered Saline Tween (TBS-T): 50 mM Tris-Cl, pH 7.5, 150 mM NaCl containing 0.05 % Tween-20

- PIPES-based buffer: 50 mM $MgSO_4$, 10 mM $CaCl_2$, 300 mM NaCl, 10 mM KCl, 10 mM PIPES, pH 6.3.

(c) Sequence characterisation

Initial primers for RACE amplification were designed from the partial cDNA sequence present in a EST database [4]. To obtain full-length sequence, new primer sets were designed for primer walking along the two isoforms. Internal PCR amplifications have also been performed to control the linearity of cloned sequences within each isoform.

To synthesise cDNA using the Superscript III Reverse Transcriptase, trizol-purified total RNA from juvenile light organs was used as a matrix, in combination with either GeneRacer RNAoligodT primers or random primers. cDNA fragments were amplified using the Platinum Taq polymerase high fidelity, following the manufacturer's instructions. The following cycling conditions were used for the RACE PCR: initial PCR: 94°C for 2 min, 5 x [94°C for 30 s, 72°C for 5 min], 5 x [94°C for 30 s, 70°C for 5 min], and 25 x [94°C for 30 s, 65°C for 30 s, 68°C for 4-6 min], 68°C for 10 min; nested PCR: 94°C for 2 min, 25 x [94°C for 30 s, 65°C for 30 s, 68°C for 4-6 min], 68°C for 10 min. For primer walking, the following conditions were used for PCR:

94°C for 5 min, 30 x [94°C for 30 s, 60°C for 30 s, 72°C for 1-7 min], 72°C for 10 min. Fragments were cloned using the 'TOPO-TA cloning kit for sequencing'. Sequencing was performed at the University of Wisconsin Biotechnology Center's DNA Sequencing Laboratory.

(d) Phylogenetic reconstruction

Hemocyanin sequences from the following mollusc species were used for tree reconstructions: *Euprymna scolopes* (this study), *Sepia officinalis* (ABD47515 and ABD47516), *Octopus = Enteroctopus dofleini* (AAU84460 and AAK28276), *Nautilus pompilius* (CAF03590), *Nucula nucleus* (CAH10286 and CAH10287), *Aplysia californica* (CAD88977), *Haliotis tuberculata* (CAC20588 and CAC82192) and *Megathura crenulata* (CAG28309 and CAG28310). Conserved sites selected by Gblocks (option: less stringent selection) represent 67% of the whole alignment (full-length protein).

(e) Gene expression

Adult and juvenile squid samples were stabilised in RNAlater, tissues were dissected and frozen at -80°C until use. Tissues for RNA extraction were homogenised using the TissueLyserLT (Qiagen) for 4 min at 30 Hz (with 5 mm stainless beads). RNA was extracted using the RNeasy kit, following the manufacturer's instructions, eluted in 30 μL of RNAse-free water (Qiagen), and incubated with TURBO DNAse for 20 min (Ambion). Reverse transcription was performed using the SMART Moloney Murine Leukemia Virus Reverse Transcriptase (MMLV RT, Clontech), starting from 500 ng of total RNA and 0.5 μg of oligo(dT)$_{12\text{-}18}$, following the manufacturer's instructions. Reaction mixes were diluted 1:8 in nanopure water before use. Negative controls were performed in the same manner but without reverse transcriptase. The

reaction mixture for quantitative RT-PCR (qRT-PCR) consisted of 0.5 μL of each primer (10 mM), 5 μL of Sso-Advanced Sybrgreen (Biorad), and 4 μL of the diluted cDNA. qRT-PCR was performed on a Biorad CFX system (2 technical replicates / biological replicate) as follows: 5 min at 95 °C, 40 times [15 s at 95 °C, 10 s at 59 °C, 15 s at 72 °C], 20 s at 70 °C. A melting curve was recorded at the end of the PCR amplification (from 70 °C to 95 °C) to confirm that a unique transcript product had been amplified. To calculate PCR efficiencies, standard curves were plotted using seven dilutions (10-10^7 copies) of a previously amplified PCR product purified using QiaQuick kit (Qiagen). Primer sets exhibit PCR efficiencies of 100.07 % ± 0.99 (99.65 % and 100.35% for *hemocyanin1* and *hemocyanin2*, respectively). Expression values were calculated by E^{-Cp}, where E corresponds to the efficiency of the PCR reaction and Cp to the crossing point [5]. Candidate gene expression was normalised by the geometric mean of the expression of three housekeeping genes (40S ribosomal protein S19, ß-tubulin and serine hydroxymethyltransferase (serine HMT)). Analysis of variance (ANOVA) residuals were checked for normality by Shapiro's test, and for homoscedasticity by Levene's test. Comparisons between aposymbiotic and symbiotic expression were performed using Tukey's HSD test (R software, version 2.14.1)

(f) Protein localisation

The peptide chosen for the antibody production is located in the functional-unit D of hemocyanin subunit 2. It was chosen for its predicted hydrophilicity and antigenicity, does not show any significant match to any sequence in the available *E. scolopes* databases nor in the non-redundant database of NCBI, and is specific to this particular functional subunit.

For the western blot procedure, one gel of 10 wells was run for the entire experiment (Mini-Protean, BioRad). The gel was cut into three sections, each section containing a set of standards. One section was stained with Coomassie as a companion gel to indicate the range of protein to which the antibody was reacting, one section was reacted with the specific antibody (α-HCY2), and the last section was reacted with the α-IgY control, because α-HCY2 antibody was produced in chicken. For blotting, proteins were transferred to PVDF membrane using a semi-dry transfer system (BioRad); the companion gel was stained with ProtoBlue Safe (National Diagnostics). Membranes were blocked overnight in Tris-Buffered Saline-Tween (TBS-T) containing 4% milk, incubated with the antibody (1:500 in TBS-T containing 1% milk) for 1 h at room temperature (RT), washed 3 times in TBS-T, incubated with goat:anti-chicken coupled to horseradish peroxidase (1:3000 in TBS-T containing 1 % milk) for 45 min at RT, and washed 3 times before visualisation by chemiluminescence (Thermo Scientific).

For ICC experiments on whole organisms, squid were incubated for 7 days with the primary antibody at a dilution of 1:1000 in blocking solution, or with IgY at the same concentration for the negative control. Samples were incubated overnight in secondary FITC-conjugated goat:anti-chicken antibody (Jackson ImmunoResearch Laboratories) at a 1:25 dilution in blocking solution. Samples were counterstained with 25 μg/mL rhodamine phalloidin in mPBST overnight for the actin cytoskeleton, and with TOTO-3 1:500 in mPBS for 20 min at room temperature for nuclei. The squid mantle cavity was opened to reveal the light organ and samples were mounted in Vectashield (Vector Laboratories) before observation by confocal microscopy to retard quenching of the fluorescence.

The embedding and sectioning for histology was provided through the Histology Laboratory, School of Veterinary Medicine, UW-Madison.

(g) Determination of oxygen affinity

Diffusion chamber experiment: The functional properties of the hemocyanins were measured with a diffusion chamber [6], using the step-by-step method [7]. The principle of this method is based on the modification of the light-absorption spectrum of a molecule when it is reversibly bound to an oxygen molecule. Briefly, a 5-µL sample is placed on a microscope slide and spread over an area of about 5 mm in diameter. The thin layer that is formed allows rapid gas exchange with the overlying gas phase. This microscope slide is placed between a light source (D2-lite) and a diode-array spectrophotometer (Ocean Optics). A flow of water vapour-saturated gas (400 mL/min) is maintained over the sample, and the proportion of oxygen in that gas flow is varied between 0 and 100%. In our experiment, the mixture of oxygen and nitrogen was controlled by mass flow-meters (MKS). The absorbance of the hemocyanin was followed at 340 nm, and recorded on a computer (acquisition of data every 5 s). For each oxygen concentration, sufficient time was given to reach equilibrium (plateau in the recording) between the gas phase and the sample (dissolved gas and oxygen bound to the hemocyanin molecules). After stables values had been obtained for 3-4 min, the proportion of oxygen could be changed again. At both the beginning and end of the experiment, absorbance values under 0 and 100% oxygen were recorded to calculate the absorbance of deoxygenated and fully oxygenated samples, respectively. This calibration also allowed us to compensate for a possible electronic drift during the experiment. We then calculated the percent saturation for each oxygen concentration step in the experiment. Throughout the experiment, the desired temperature was maintained by a water jacket surrounding the whole system including the sample, humidifying chambers, and tubing carrying the gas mixture, once it was saturated with water vapour.

Preparation of the samples: The protein concentration from either native hemolymph or 'purified' hemocyanin samples was determined before the washing step by the Bradford method. The pH values were varied by mixing 15 μL of each sample to 5 μL of 500 mM Tris, 375 mM NaCl, adjusted at the desired pH (final concentrations of the diluted sample: 25 mM Tris, 375 mM NaCl, 11 mM $CaCl_2$, 45 mM $MgCl_2$, 11.25 mM KCl). The pH of the native samples and the pH-adjusted samples were measured by an Orion 3-Star pH-meter equipped with a needle microelectrode (Thermo). Five μL of these pH-adjusted samples were placed on the microscope slide.

Analysis of raw diffusion chamber data: The experiment allowed us to collect absorbance data for different proportions of oxygen, and to calculate the saturation of the hemocyanin for each. The relationship between the saturation (S) and the partial pressure of oxygen (PO_2) was transformed and plotted as log (S/1-S)=f(log PO_2) (Hill transform). From the typical sigmoid shape of the S=f(PO_2) plot, the relationship becomes linear between 30 and 70 % saturation (*e.g.,* see [8]). At 50 % saturation, the line intercepts the X-axis at the value log (P_{50}), where P_{50} is the partial pressure of oxygen necessary to saturate half of the molecules (*i.e.*, a higher P_{50} reflects a lower affinity). The slope of this portion of the curve corresponds to the Hill coefficient (n_{50}, the cooperativity coefficient around 50 % of saturation). Towards greater and lower saturation values, the relationship is no longer linear, and inflects to reach a slope of 1. We however did not need to explore theses states of saturation for the present study, as they do not affect the ability to calculate P_{50} and n_{50}. For each condition, at least 4 data points were used to calculate these parameters. The correlation coefficient was always greater than 0.99, allowing reliable calculation of the intercept and slope parameters.

The reversible binding of oxygen by hemocyanin can induce the release of a proton, and pH can therefore affect the binding equilibrium. This effect is called the Bohr effect, and is quantified by $\Phi = \Delta \log P_{50}/\Delta pH$. This effect may not be constant with pH, and is reported with the value of pH around which it was calculated.

(h) Antimicrobial activity

Bacteria were grown in seawater tryptone (SWT) medium overnight, and a fresh culture was started from a 1:1000 dilution before the experiment. Two-fold dilutions of hemocyanin were performed in a final volume of 90 μL in a 96-well plate. When OD_{600} reached 0.1-0.2, a subset of the bacterial culture was diluted in SWT to obtain 10 colony-forming units (CFU)/μL, and 10 μL were dispensed in each well, except for wells designated as sterile controls. Experiments were run in triplicate.

The Gram-positive strains used in this study (CNJ 771, CNJ 778 and CNJ 803) have been kindly provided by Paul Jensen [9]. All the other strains have been isolated from Hawaiian seawater. The correspondence between OD_{600} and CFU was the following:

1 OD = 2×10^8 CFU (ES114, KNH1, NK_St13, Lna)

1 OD = 1.4×10^8 CFU (CNJ 771)

1 OD = 1.08×10^7 CFU (CNJ 778)

1 OD = 1.25×10^8 (CNJ 803)

Supplementary figure legends:

Supplementary table T1: Primers used for molecular studies

Supplementary figure S1: Sequence characterisation of both hemocyanin subunits

(*a*) Alignment of hemocyanin functional units from the two isoforms described in *Euprymna scolopes* (this study) and *Sepia officinalis* (ABD47515 and ABD47516). Secondary structure is based on a previous study [10]. Conserved residues were determined in comparison with *Octopus dofleini* [11], *Haliotis tuberculata* [12] and *Nucula nucleus* [13]. *N*-glycosylation sites were predicted by NetNGlyc 1.0 (http://www.cbs.dtu.dk/services/NetNGlyc/) (threshold > 0.5) and copper-binding sites were derived from a previous review [14].

(*b*) Phylogenetic reconstruction of hemocyanin functional units by Maximum Likelihood inference. Data from different molluscan species were used for the reconstruction: *Euprymna* = *E. scolopes* (this study), *Sepia* = *S. officinalis* (ABD47515 and ABD47516), *Octopus* = *Enteroctopus dofleini* (AAU84460 and AAK28276), *Nautilus* = *N. pompilius* (CAF03590), *Nucula* = *N. nucleus* (CAH10286 and CAH10287), *Aplysia* = *A. californica* (CAD88977), *Haliotis* = *H. tuberculata* (CAC20588 and CAC82192) and *Megatura* = *M. crenulata* (CAG28309 and CAG28310). Alignment was performed using Muscle v3.7 [15], and manually checked using Seaview [16]; informative sites were selected using Gblocks v0.91b (option: less stringent selection) [17], and the phylogeny was reconstructed using PhyML v3.0 [18] with the WAG+Γ model, and 100 bootstrap replicates were conducted for support estimation (dryad doi: 10.5061/dryad.cq032). The interface from phlygeny.fr was used as a platform for the reconstruction [19].

Supplementary figure S2: Negative controls of ISH, western blot and ICC

(*a*) *In situ* hybridisation of *Eshcy2* (sense probe). No staining was visible in the gills.

(*b*) Coomassie staining of a 7 % acrylamide SDS-PAGE gel (right) of soluble-protein extracts from juvenile light organs, and its associated western blot (left) against control α-IgY (GenScript). IgY was used as a control because the polyclonal antibody (α-HCY2) was generated in chicken.

(*c-g*) Immunocytochemistry of juvenile tissues against control IgY (GenScript). No staining was visible in the gills (*c*), the ciliated field (*d*), the cytosol of the appendage epithelium (*e*), or in the pores/duct region (*g*). Green, α-IgY; red, rhodamine phalloidin (f-actin); blue, TOTO-3 (nuclei).

(*f*) Immunocytochemistry using control IgY (GenScript) in the mucus coating the appendage epithelium. Green, α-IgY; blue, Alexa633-WGA (mucus-binding lectin wheat-germ agglutinin).

(*h-i*) Immunocytochemistry using control IgY on 5-μm sections of juvenile (*h*) and adult (*i*) light organs. Green, α-IgY; red, rhodamine phalloidin (f-actin); blue, TOTO-3 (nuclei). The inset shows α-IgY staining (green channel only) corresponding to the dotted area.

Supplementary figure S3: Localisation of hemocyanin in the light organ, during various symbiotic conditions and over the day/night cycle

(*a*) Scheme representing the natural diel variation in bacterial content in the light organ over the day/night cycle in symbiotic *E. scolopes* squid.

(*b*) Immunocytochemistry against *Es*HCY2 on 5-μm sections of juvenile (48 h, equivalent of noon in adult's schedule) or adult crypts. Samples from aposymbiotic, as well as symbiotic-WT

and symbiotic-Lux* (Δ*lux*) colonized squid were tested. Note that the Δ*lux* symbionts have been eliminated from the light organ by 4 weeks post-inoculation. Green, α-HCY2; red, rhodamine phalloidin (f-actin); blue, TOTO-3 (nuclei). Scale bar = 20 μm.

(*c*) Immunocytochemistry of control IgY on 5-μm sections of juvenile (48 h) or adult crypts. Green, α-IgY; red, rhodamine phalloidin (f-actin); blue, TOTO-3 (nuclei). Scale bar = 20 μm

Supplementary figure S4: Cooperativity of hemocyanin, and influence of buffers and organic components on oxygen affinity

(*a*) Cooperativity (n_{50}) of either native hemolymph, adjusted with Tris buffer (left), or the hemocyanin alone, washed in Tris buffer to remove other hemolymph components (right) determined at different pH values.

(*b*) The Bohr effect of hemocyanin washed with different buffer solutions. Tris: 500 mM Tris, 375 mM NaCl; HEPES: 300 mM HEPES, 375 mM NaCl; Imidazole: 500 mM Imidazole, 375 mM NaCl. The P_{50} values are reported in kPa.

(*c*) Influence of added organic components believed to be present in the crypt space on hemocyanin affinity and cooperativity at pH = 7 (Tris buffer). The P_{50} values are reported in kPa.

Supplementary figure S5: Procedure for hemocyanin purification, and determination of phenol oxidase activity against tyramine and catechol.

(*a*) The purification pipeline of *Es*HCY is illustrated (top), and followed both by the elution profile from the anion exchange HPLC (left) and by an SDS-PAGE gel of samples extracted at different stages during the purification process (right). The predicted pI for HCY1 and HCY2 are 5.65 and 5.73, respectively. The HPLC procedure separated two main peaks of hemocyanin (# I

and # II), which were pooled for further experiments. For the SDS-PAGE, samples were run on a NuPage Novex 4-12 % gradient gel (with or without denaturation by Tris-(2-carboxyethyl)-phosphine hydrochloride (TCEP, ThermoScientific) and 95 °C incubation for 10 min), and stained with Sypro Ruby (Invitrogen). Characterisation of several bands (squared) was performed by mass spectrometry at the UW-Madison Biotechnology Center.

(*b*) Phenol oxidase activity of purified *Es*HCY (same experimental conditions used for dopamine, Figure 4): Cresolase activity against 3.4 mM tyramine (left) and catecholase activity against 6 mM catechol (right) after incubation with proteases.

References associated with the supplementary material:

1 Boettcher KJ, Ruby EG. 1990 Depressed light emission by symbiotic *Vibrio fischeri* of the sepiolid squid *Euprymna scolopes*. *J. Bacteriol.* **172**, 3701–3706.

2 Bose JL, Rosenberg CS, Stabb EV. 2008 Effects of luxCDABEG induction in *Vibrio fischeri:* enhancement of symbiotic colonization and conditional attenuation of growth in culture. *Arch. Microbiol.* **190**, 169–83. (doi:10.1007/s00203-008-0387-1)

3 Nyholm SV, Stewart JJ, Ruby EG, McFall-Ngai MJ. 2009 Recognition between symbiotic *Vibrio fischeri* and the haemocytes of *Euprymna scolopes*. *Environ. Microbiol.* **11**, 483–493. (doi:10.1111/j.1462-2920.2008.01788.x)

4 Chun CK *et al*. 2006 An annotated cDNA library of juvenile *Euprymna scolopes* with and without colonization by the symbiont *Vibrio fischeri*. *BMC Genomics* **7**, 154. (doi:10.1186/1471-2164-7-154)

5 Pfaffl MW. 2001 A new mathematical model for relative quantification in real-time RT-PCR. *Nucleic Acids Res* **29**, e45.

6 Sick H, Gersonde K. 1969 Method for continuous registration of O_2-binding curves of hemoproteins by means of a diffusion chamber. *Anal. Biochem.* **32**, 362–76.

7 Weber RE. 1981 Cationic control of O_2 affinity in lugworm erythrocruorin. *Nature* **292**, 386–387. (doi:10.1038/292386a0)

8 Toulmond A, El Idrissi Slitine F, De Frescheville J, Jouin C. 1990 Extracellular hemoglobins of hydrothermal vent annelids : structural and functional characteristics in three alvinellid species. *Biol. Bull.* **179**, 366–373.

9 Gontang EA, Fenical W, Jensen PR. 2007 Phylogenetic diversity of gram-positive bacteria cultured from marine sediments. *Appl. Environ. Microbiol.* **73**, 3272–82. (doi:10.1128/AEM.02811-06)

10 Cuff ME, Miller KI, van Holde KE, Hendrickson WA. 1998 Crystal structure of a functional unit from *Octopus* hemocyanin. *J. Mol. Biol.* **278**, 855–870. (doi:10.1006/jmbi.1998.1647)

11 Miller KI, Cuff ME, Lang WF, Varga-Weisz P, Field KG, van Holde KE. 1998 Sequence of the *Octopus dofleini* hemocyanin subunit: structural and evolutionary implications. *J. Mol. Biol.* **278**, 827–42. (doi:10.1006/jmbi.1998.1648)

12 Lieb B, Altenhein B, Markl J. 2000 The sequence of a gastropod hemocyanin (HtH1 from *Haliotis tuberculata*). *J. Biol. Chem.* **275**, 5675–5681.

13 Bergmann S, Markl J, Lieb B. 2007 The first complete cDNA sequence of the hemocyanin from a bivalve, the protobranch *Nucula nucleus*. *J. Mol. Evol.* **64**, 500–510. (doi:10.1007/s00239-006-0036-8)

14 Van Holde KE, Miller KI, Decker H. 2001 Hemocyanins and invertebrate evolution. *J. Biol. Chem.* **276**, 15563–6. (doi:10.1074/jbc.R100010200)

15 Edgar RC, Drive RM, Valley M. 2004 MUSCLE : multiple sequence alignment with high accuracy and high throughput. *BMC Bioinformatics* **32**, 1792–1797. (doi:10.1093/nar/gkh340)

16 Gouy M, Guindon S, Gascuel O. 2010 SeaView version 4: A multiplatform graphical user interface for sequence alignment and phylogenetic tree building. *Mol. Biol. Evol.* **27**, 221–4. (doi:10.1093/molbev/msp259)

17 Castresana J. 2000 Selection of conserved blocks from multiple alignments for their use in phylogenetic analysis. *Mol. Biol. Evol.* **17**, 540–552.

18 Guindon S, Gascuel O. 2003 A simple, fast, and accurate algorithm to estimate large phylogenies by maximum likelihood. *Syst. Biol.* **52**, 696–704. (doi:10.1080/10635150390235520)

19 Dereeper A *et al*. 2008 Phylogeny.fr: robust phylogenetic analysis for the non-specialist. *Nucleic Acids Res.* **36**, W465–9. (doi:10.1093/nar/gkn180)

Supplementary table 1

	Primer Name	Sequence	Product size (bp)
ISH		Hemocyanin subunit 1	395
	Hem1-HIS-F	CCACGACCGTCTAACATACG	
	Hem1-HIS-R	CGCCGATCACTTCTGTCTTA	
	Hem1-T7-HIS-F	TAA TAC GAC TCA CTA TAG GGCCACGACCGTCTAACATACG	
	Hem1-T7-HIS-R	TAA TAC GAC TCA CTA TAG GGCGCCGATCACTTCTGTCTTA	
		Hemocyanin subunit 2	393
	Hem2-HIS-F	GATGGCAGATGAAGGTCGAT	
	Hem2-HIS-R	AACACGAAGAGGGTGTGGTC	
	Hem2-T7-HIS-F	TAA TAC GAC TCA CTA TAG GGGATGGCAGATGAAGGTCGAT	
	Hem2-T7-HIS-R	TAA TAC GAC TCA CTA TAG GGAACACGAAGAGGGTGTGGTC	
qRT-PCR		Hemocyanin subunit 1	136
	HemS1-qF	GGTCCAGGTCGGCATTACTA	
	HemS1-qR	TTCCTCCATTGGAAATCAGC	
		Hemocyanin subunit 2	157
	HemS2-qF	ATTTGGCGGTACCTTCTGTG	
	HemS2-qR	GCCGTCGATACCCATAATTG	

Supplementary figure 1

(*a*)

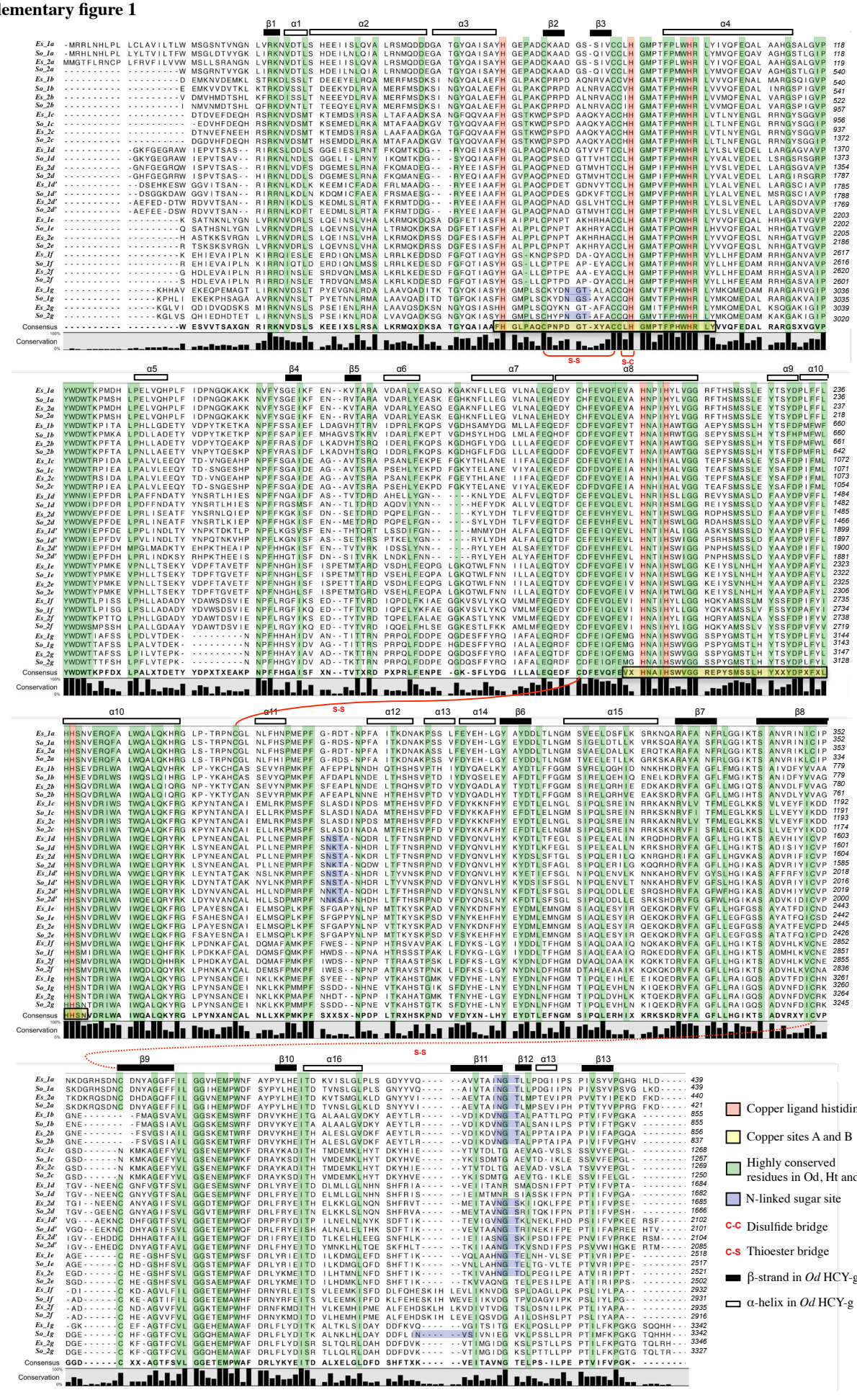

(*b*)

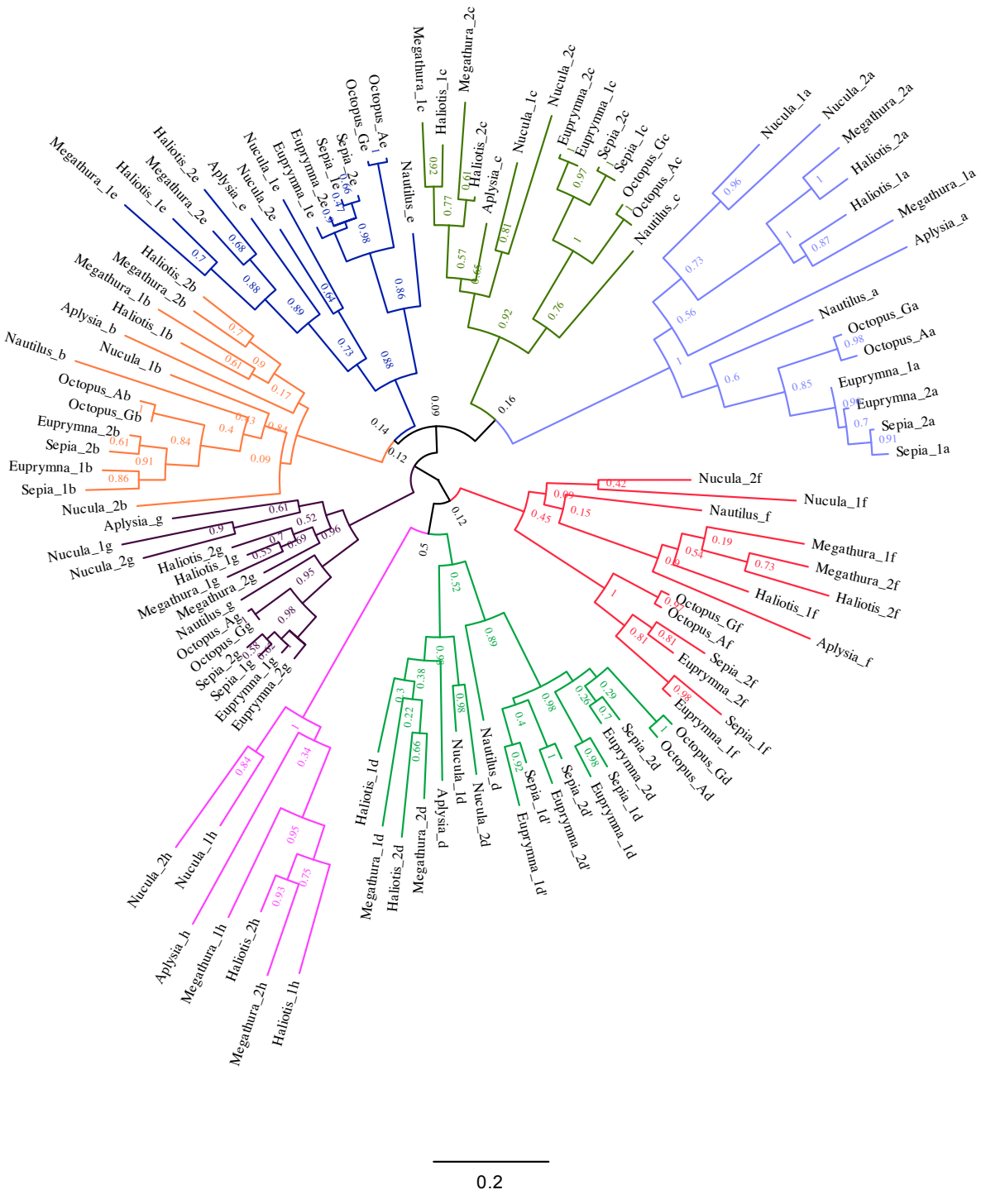
Megathura_1c
Haliotis_1c
Megathura_2c
Octopus_Ae
Octopus_Ge
Nautilus_e
Haliotis_2c
Nucula_1c
Nucula_2c
Euprymna_2c
Euprymna_1c
Sepia_2c
Sepia_1c
Octopus_Gc
Octopus_Ac
Nautilus_c
Nucula_1a
Nucula_2a
Megathura_2a
Haliotis_2a
Haliotis_1a
Megathura_1a
Aplysia_a
Nautilus_a
Octopus_Ga
Octopus_Aa
Euprymna_1a
Euprymna_2a
Sepia_2a
Sepia_1a
Megathura_1e
Haliotis_1e
Haliotis_2e
Megathura_2e
Aplysia_e
Nucula_1e
Nucula_2e
Euprymna_1e
Euprymna_2e
Sepia_1e
Sepia_2e
Haliotis_2b
Megathura_2b
Megathura_1b
Haliotis_1b
Aplysia_b
Nucula_1b
Nautilus_b
Octopus_Ab
Octopus_Gb
Euprymna_2b
Sepia_2b
Euprymna_1b
Sepia_1b
Nucula_2b
Aplysia_g
Nucula_1g
Nucula_2g
Haliotis_2g
Haliotis_1g
Megathura_1g
Megathura_2g
Nautilus_g
Octopus_Ag
Octopus_Gg
Sepia_2g
Sepia_1g
Euprymna_1g
Euprymna_2g
Nucula_2f
Nucula_1f
Nautilus_f
Megathura_1f
Megathura_2f
Haliotis_1f
Haliotis_2f
Aplysia_f
Octopus_Gf
Octopus_Af
Sepia_2f
Euprymna_2f
Sepia_1f
Euprymna_1f
Octopus_Gd
Octopus_Ad
Sepia_2d
Euprymna_2d
Sepia_1d
Euprymna_1d
Sepia_2d'
Euprymna_2d'
Sepia_1d'
Euprymna_1d'
Nautilus_d
Nucula_2d
Nucula_1d
Aplysia_d
Megathura_2d
Haliotis_2d
Haliotis_1d
Megathura_1d
Nucula_2h
Nucula_1h
Aplysia_h
Megathura_1h
Haliotis_2h
Megathura_2h
Haliotis_1h
0.2

Supplementary Figure 2

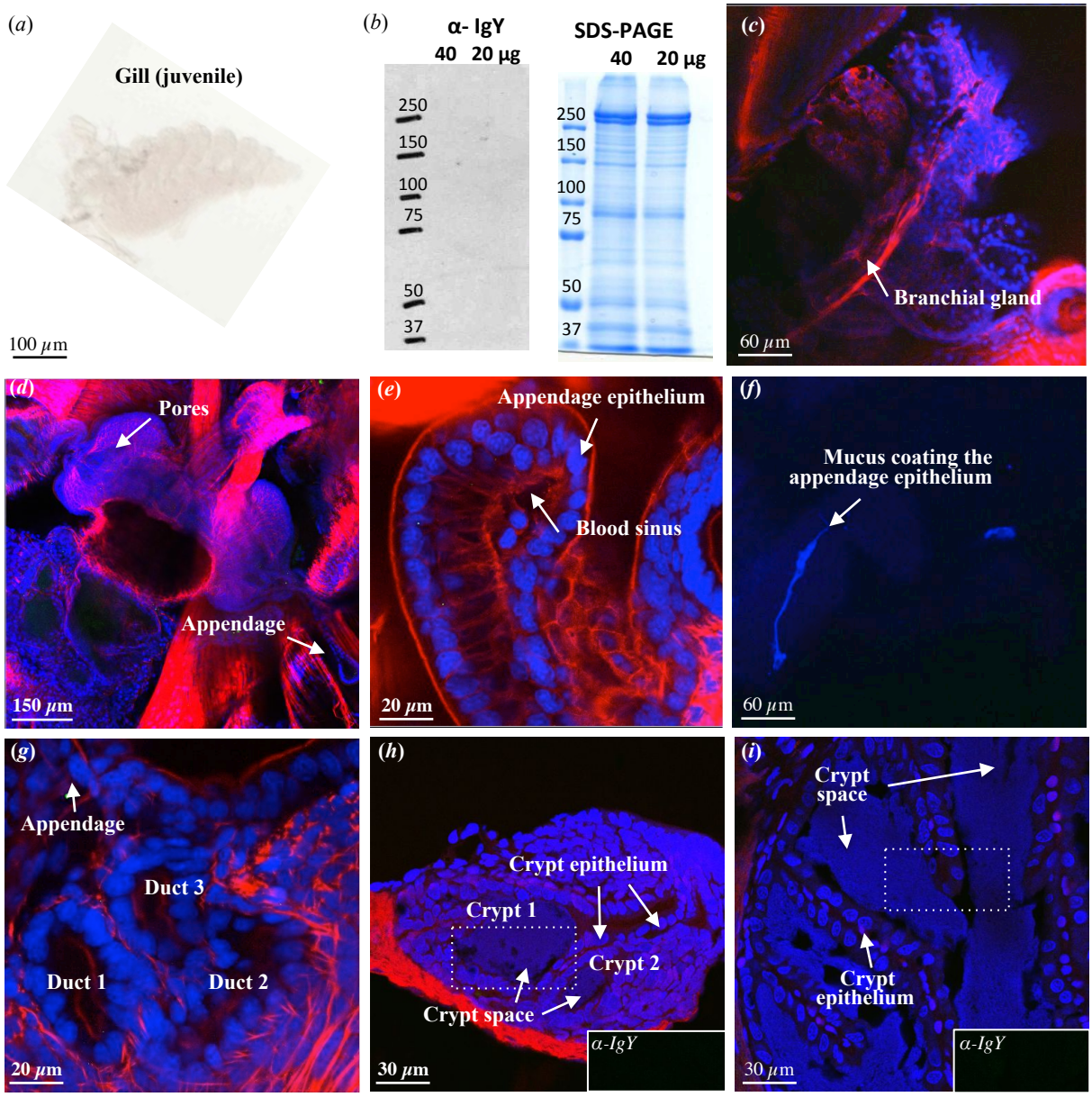

Supplementary Figure 3

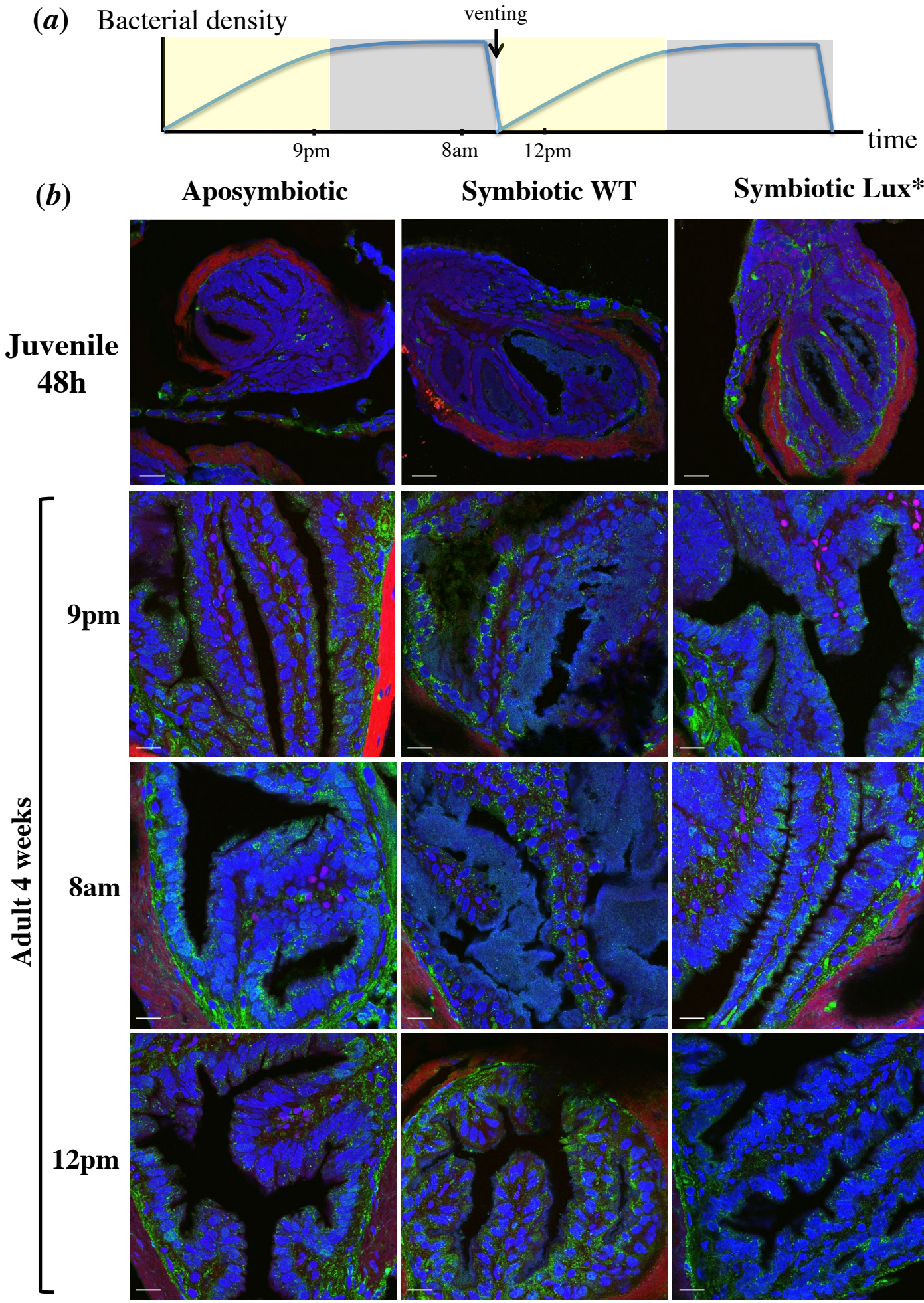

(*c*) Negative controls

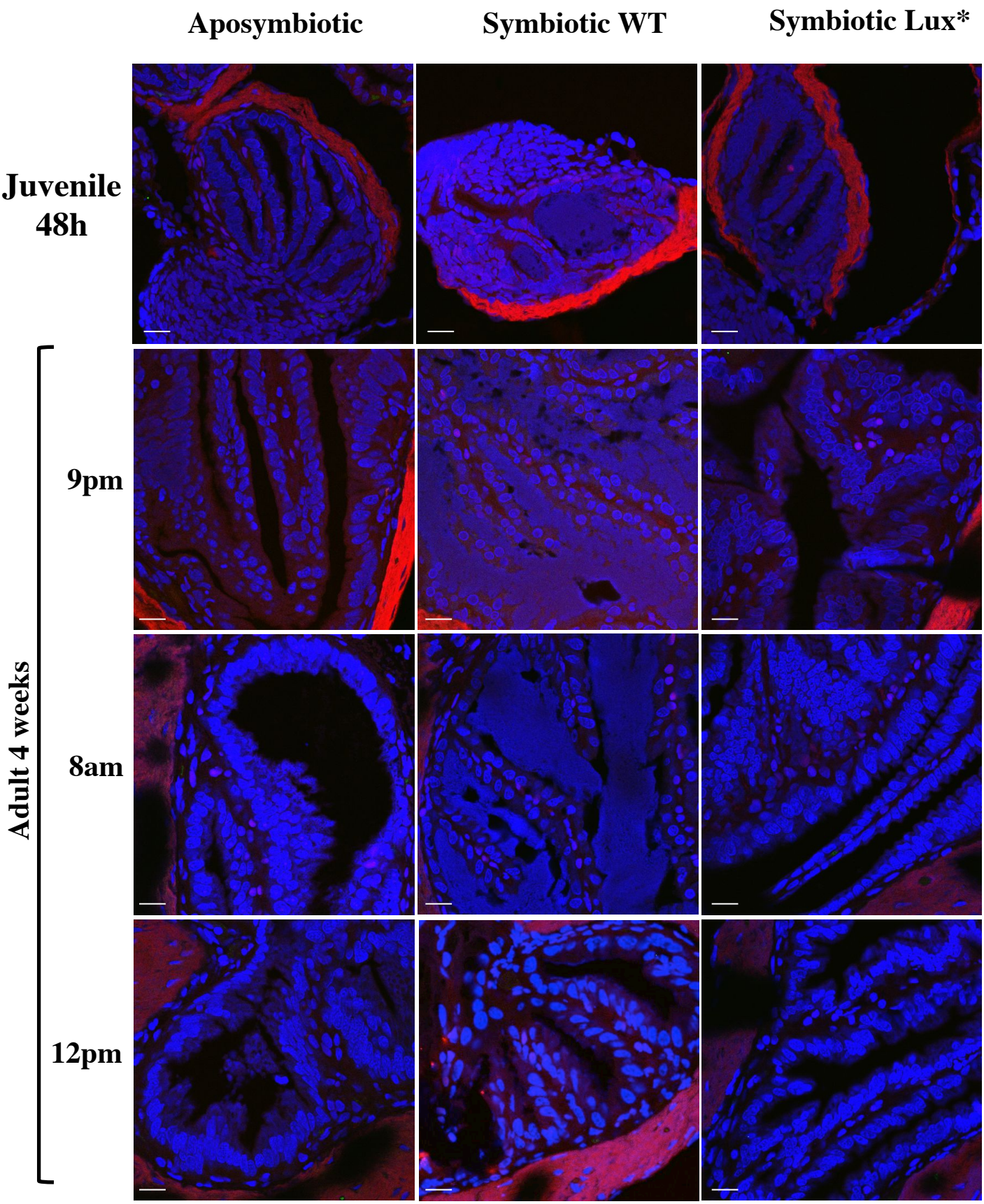

Supplementary Figure 4

(*a*)

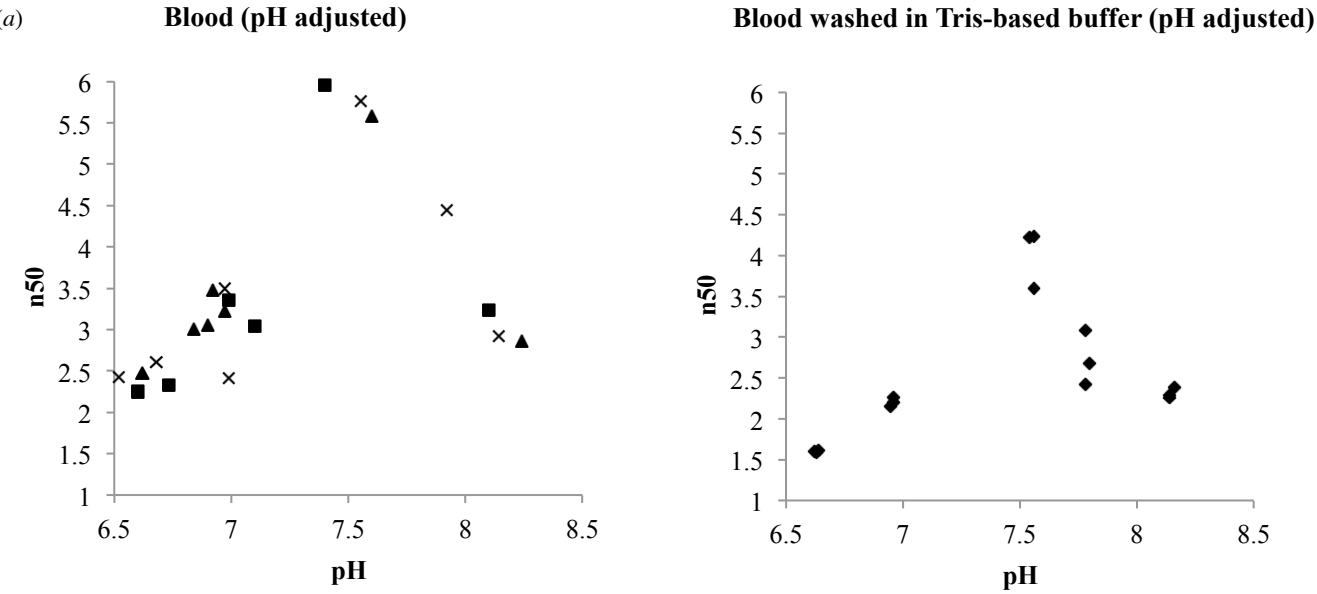

(*b*)

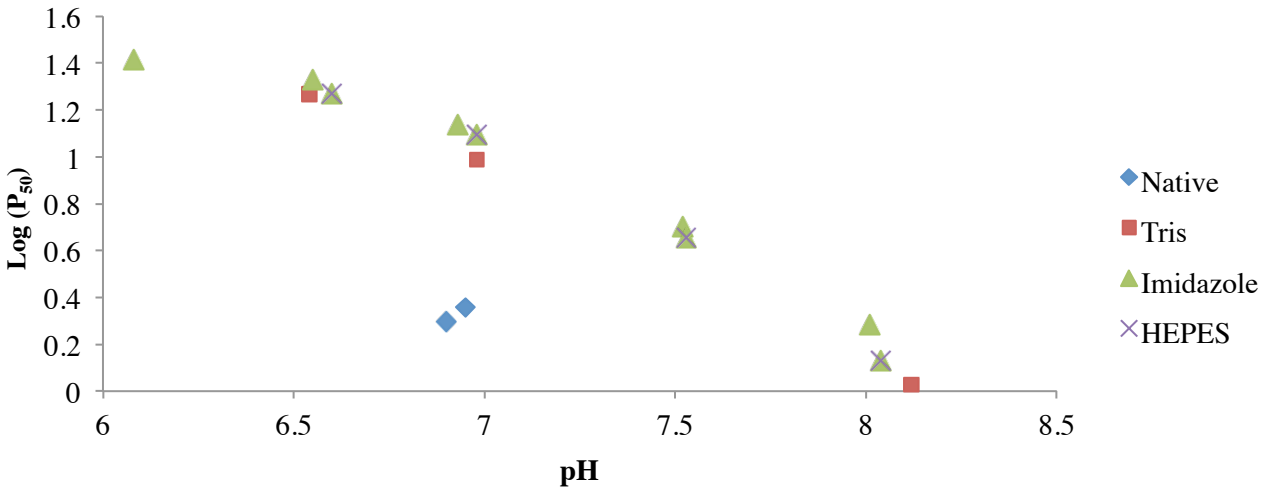

(*c*)

Experimental condition	pH	p50	log p50	n50
HCY (native conditions)	6.85	3.31	0.52	2.19
HCY washed in Tris buffer (H-T)	6.98	11.48	1.06	2.28
H-T + Acetate 0.1 mM	6.95	11.99	1.08	2.31
H-T + Acetate 1 mM	6.97	12.08	1.08	2.27
H-T + Acetate 10 mM	6.96	12.14	1.08	2.33
H-T + Lactate 0.1 mM	6.99	11.97	1.08	2.2
H-T + Lactate 1 mM	6.99	12.19	1.09	2.21
H-T + Lactate 10 mM	6.95	11.45	1.06	2.13
H-T + Taurine 1 mM	6.95	11.63	1.07	2.11
H-T + Taurine 10 mM	6.97	10.94	1.04	2.10

Supplementary figure 5

(*a*)

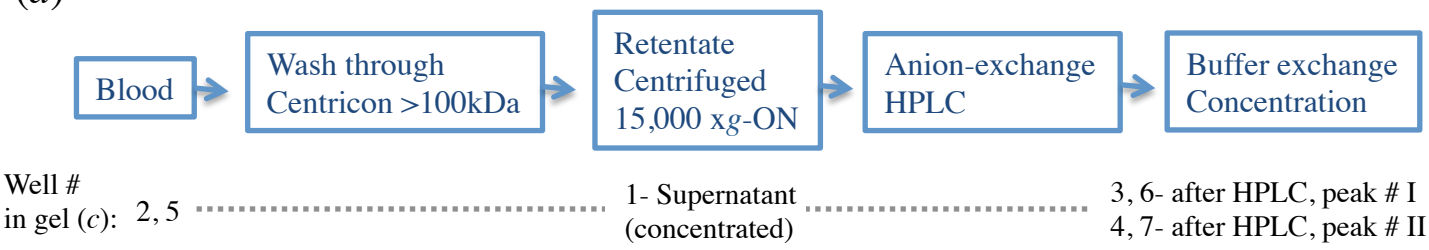

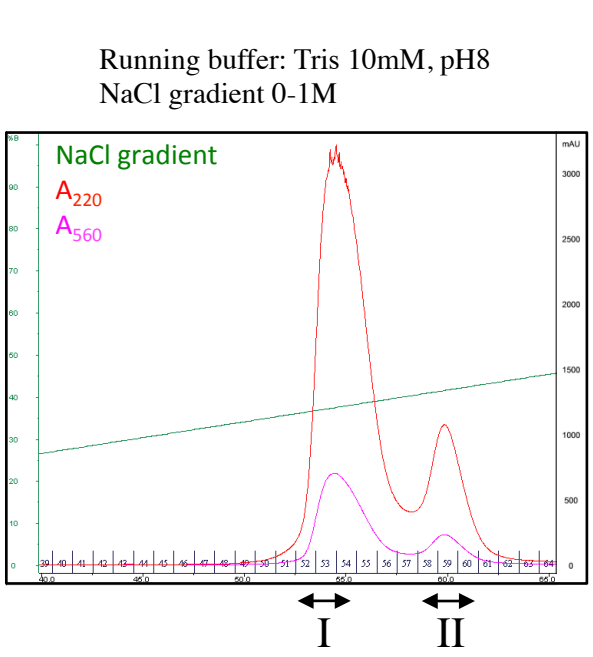

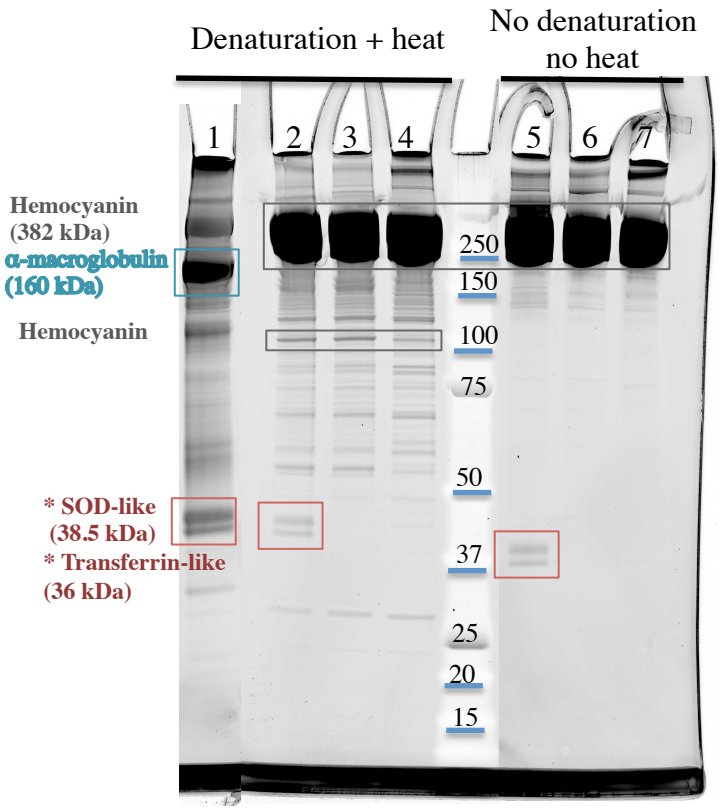

(*b*)